INVESTIGATIONS OF AXIAL FUEL SHUFFLING SCHEMES FOR A HIGH-TEMPERATURE GAS-COOLED REACTOR

A THESIS

Presented to

The Faculty of the Division of Graduate

Studies and Research

by

David Fulton Hoppes

In Partial Fulfillment

of the Requirements for the Degree

Master of Science in Nuclear Engineering

Georgia Institute of Technology

March, 1972

In presenting the dissertation as a partial fulfillment of the requirements for an advanced degree from the Georgia Institute of Technology, I agree that the Library of the Institute shall make it available for inspection and circulation in accordance with its regulations governing materials of this type. I agree that permission to copy from, or to publish from, this dissertation may be granted by the professor under whose direction it was written, or, in his absence, by the Dean of the Graduate Division when such copying or publication is solely for scholarly purposes and does not involve potential financial gain. It is understood that any copying from, or publication of, this dissertation which involves potential financial gain will not be allowed without written permission.

_____

7/25/68

INVESTIGATIONS OF AXIAL FUEL SHUFFLING SCHEMES

FOR A HIGH-TEMPERATURE GAS-COOLED REACTOR

Approved: [signature]

Date approved by Chairman: Feb. 23, '72

ACKNOWLEDGMENTS

I would like to acknowledge the assistance of some of the people who have had an interest in this thesis project. My adviser, Dr. R. J. Johnson, was instrumental in setting up communications with the Gulf General Atomic Company, as well as offering technical help. He and the other members of the reading committee, Dr. J. M. Kallfelz, Dr. S. C. Barnett, and Dr. W. W. Graham, provided considerable assistance in the drafting of this thesis. I am also indebted to Dr. A. Shenoy and Dr. R. Brogli, both of Gulf General Atomic Company, for their invaluable help with this project. I would also like to acknowledge the financial support which I have received through an Atomic Energy Commission Traineeship in Nuclear Engineering while working on this thesis.

TABLE OF CONTENTS

LIST OF TABLES

LIST OF ILLUSTRATIONS

CHAPTER I

INTRODUCTION

Statement of the Problem

This project had as its goal the optimization of an equilibrium fuel scheme for a 1100 MW(e) high-temperature gas-cooled reactor (HTGR) which has been designed by Gulf General Atomic (GGA) Company. This fuel scheme is to be adaptable to an HTGR which can be used for coal-gasification and other process heat applications as well as power production.

Two computer codes furnished by GGA were used in this investigation. The code FEVER[1] was used to calculate the time-dependent nuclide concentrations, K_{eff} values and power distributions in the reactor core. It was used in an attempt to find the fuel composition for an acceptable fuel scheme. The code POKE[2] is a thermal and flow analysis routine for gas-cooled reactors. It was used to analyze several of the better fuel schemes to determine the resulting core temperature distributions.

From the standpoint of this project, the most significant feature of the HTGR fuel system is that fuel elements can be rearranged, or "shuffled," in the axial direction at each refueling. The active core contains eight layers of fuel elements in the axial direction. For a four year fuel cycle, one-fourth of the core fuel is replaced yearly. At equilibrium fuel cycle conditions, which are approximated after four to five years of reactor operation, approximately the same fresh fuel concentrations are added yearly and the same depleted fuel concentrations are

removed yearly. Only one equilibrium axial-shuffling method was investigated in this project, an "axial push through" scheme. In this scheme, two fresh fuel elements are added yearly at the top of each axial fuel column, each of the elements already present in the column is moved two axial positions lower, and the two oldest fuel elements (with four year core residence time) are removed from the bottom of the core. Thus, immediately after refueling the top two axial fuel layers are occupied by fresh fuel, the third and fourth layers contain one-year old fuel, the fifth and sixth layers contain two-year old fuel, and the bottom two layers contain three-year old fuel. It is hoped that an axial push through fuel scheme, with the proper choice of fuel composition, will result in an approximately exponential power distribution with the peak power level at the top of the core. As will be shown, such a power distribution leads to the ideal flat center-line fuel temperature profile in the axial direction.

It is important to note that nearly all light-water reactors employ radial, rather than axial, fuel shuffling. In the case of most light-water reactors, axial fuel shuffle would not be possible as the unsegmented fuel rods extend the total length of the core. In radial fuel shuffling, the total fuel assembly is shuffled from one radial position to another, with a principal objective being a relatively flat power profile in the radial direction.

Some of the important reactor parameters which were assumed to be fixed for the purpose of this project were: reactor power level, coolant inlet temperature, core geometry and size, fuel cycle time, and in-core

fuel lifetime. The variables in this project were the nuclide concentrations of the fresh fuel.

The overriding requirement for a fuel scheme is that it have a relatively flat fuel temperature profile, with maximum fuel temperatures below a level specified by material limitations. Ideally, all the fuel would operate at a temperature which is slightly below the specified level. This would produce the maximum allowable gas outlet temperature, while not impairing the integrity of the fuel material. The generation of a very high gas outlet temperature is a prime requirement for process heat applications. Other important criteria for the fuel scheme are the stability of the axial power distribution during burnup, and the behavior of the power distribution when control rods are partially withdrawn. As the initial fully-fueled core is depleted, it becomes necessary to withdraw control rods throughout the year to compensate for the loss of reactivity. The fuel scheme must have an acceptable power distribution which is relatively constant during core burnup, as the control rods are being withdrawn to the upper levels of the core. An acceptable power distribution insures an acceptable fuel temperature profile. The investigation procedure used and the results obtained are discussed in Chapter III.

Description of the High-Temperature Gas-Cooled Reactor (HTGR) System

The HTGR is a graphite-moderated helium-cooled reactor in which graphite serves as moderator, reflector, and core structure. The fuel cycle includes thorium (Th^{232}) as a fertile material. The bred U^{233} is recycled, in the final equilibrium fuel cycle, to provide fissile fuel material along with enriched U^{235} which is added as required for makeup.

The general reactor arrangement is shown in Figure 1. The entire primary cooling system, including steam generators and helium circulators, and the reactor core are contained within a prestressed-concrete reactor pressure vessel (PCRV). The helium is heated during downward flow through the core by passing through coolant channels in the fuel elements. The helium is then directed to steam generators, where heat is transferred to the secondary (steam) coolant. The steam is sent from the PCRV to process heat applications or to a turbine-generator plant. The helium then flows from the steam generator to circulator inlets. From the circulator discharge, the cooled helium flows upward in the annular space between the core barrel and the inner surface of the PCRV liner into a plenum above the reactor core. From there it flows downward through the core.

The prestressed concrete in the PCRV serves as the structure to contain the primary coolant pressure (about 700 psia), and a steel liner serves as a gastight membrane.[3] Nearly absolute leaktightness of the steel membrane is required for the plant's 30-year life without provision for maintenance. Thermal protection for the vessel is provided by insulation inside the liner and by water cooling on the outside of the liner.

For a 1100 MW(e) plant there are six steam-generator modules; each consists of three tube bundles: a reheater section, a superheater section, and an economizer-evaporator section. The tubes are arranged in a series of concentric helical coils. The helium flows over a matrix of in-line tubes, with steam on the tube side. The helium which is discharged from the six steam-generators is moved through three primary helium circulation loops, and returns to a plenum above the core.

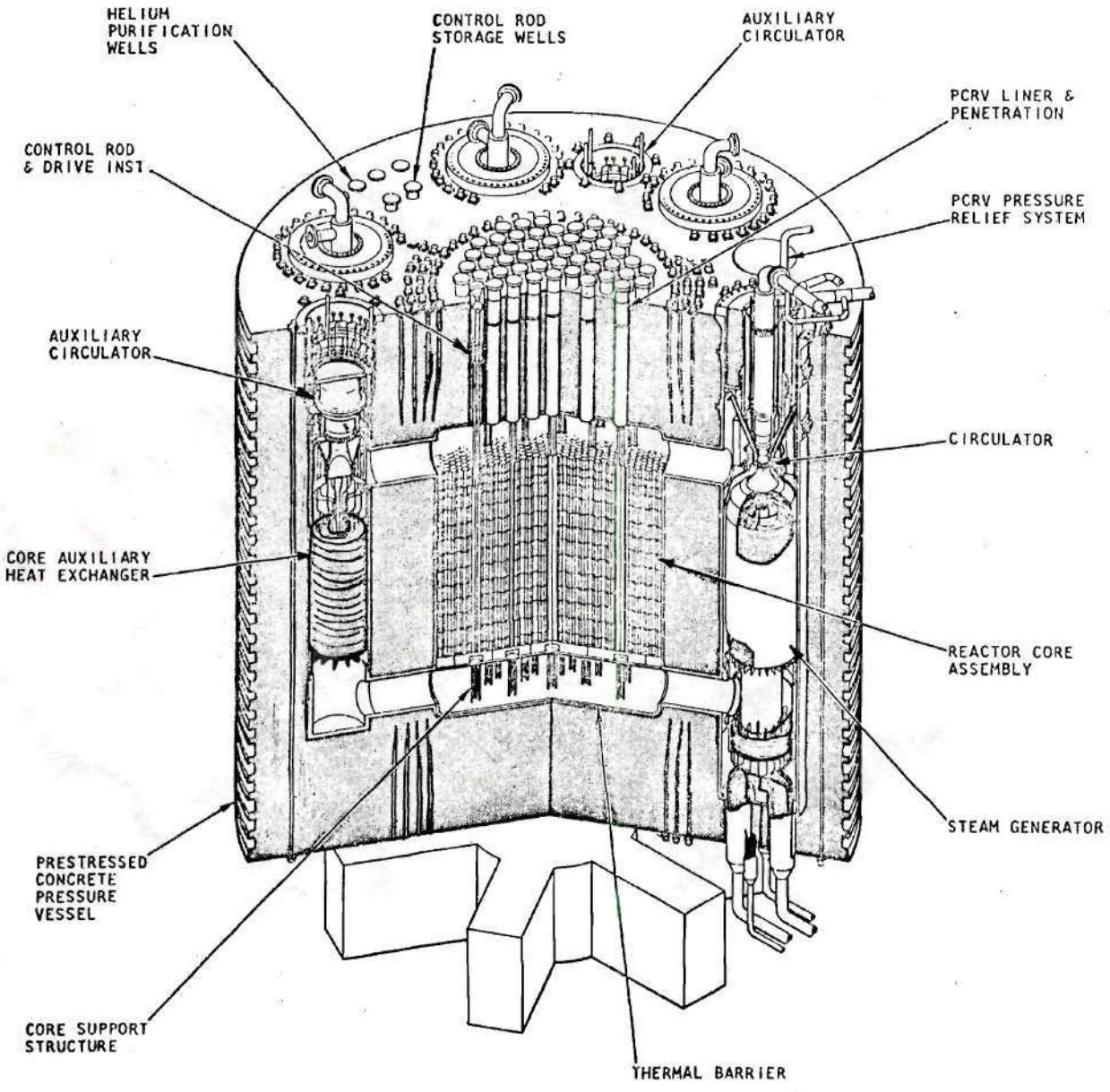

Figure 1. General Reactor Arrangement

HTGR Core[4]

The core for the proposed 1100 MW(e) HTGR is basically an extrapolation from the design of the Fort St. Vrain reactor, which is scheduled to begin operation early in 1972. The reactor core consists of vertical columns of hexagonal graphite fuel-moderator elements and graphite reflector blocks grouped into a cylindrical array and supported by a graphite core support structure. There is no separate moderator or structural material in the active core apart from that in the removable fuel elements. The plan view of the core is divided into 73 radial fuel regions, normally consisting of a central fuel element column with six surrounding fuel columns. This is shown in Figure 2. Control rod and reserve shutdown channels are provided within the central fuel element of each radial fuel region. The basic core specifications and performance criteria for an HTGR applicable to process heat applications are summarized in Table 1. Figure 3 shows the core arrangement.

The next section will describe the core fuel system, with the control system and burnable poisons considered as they apply to the fuel system.

Fuel Particles

The most elemental constituents of the fuel system are coated fuel particles, of which there are two basic types: fissile (uranium) and fertile (thorium). These fuel particles are bonded together in a graphite matrix to form fuel rods; the rods are grouped together in the hexagonal fuel elements which were shown in preceding figures.

The fuel particles consist of a kernal of metal carbide, UC_2 or

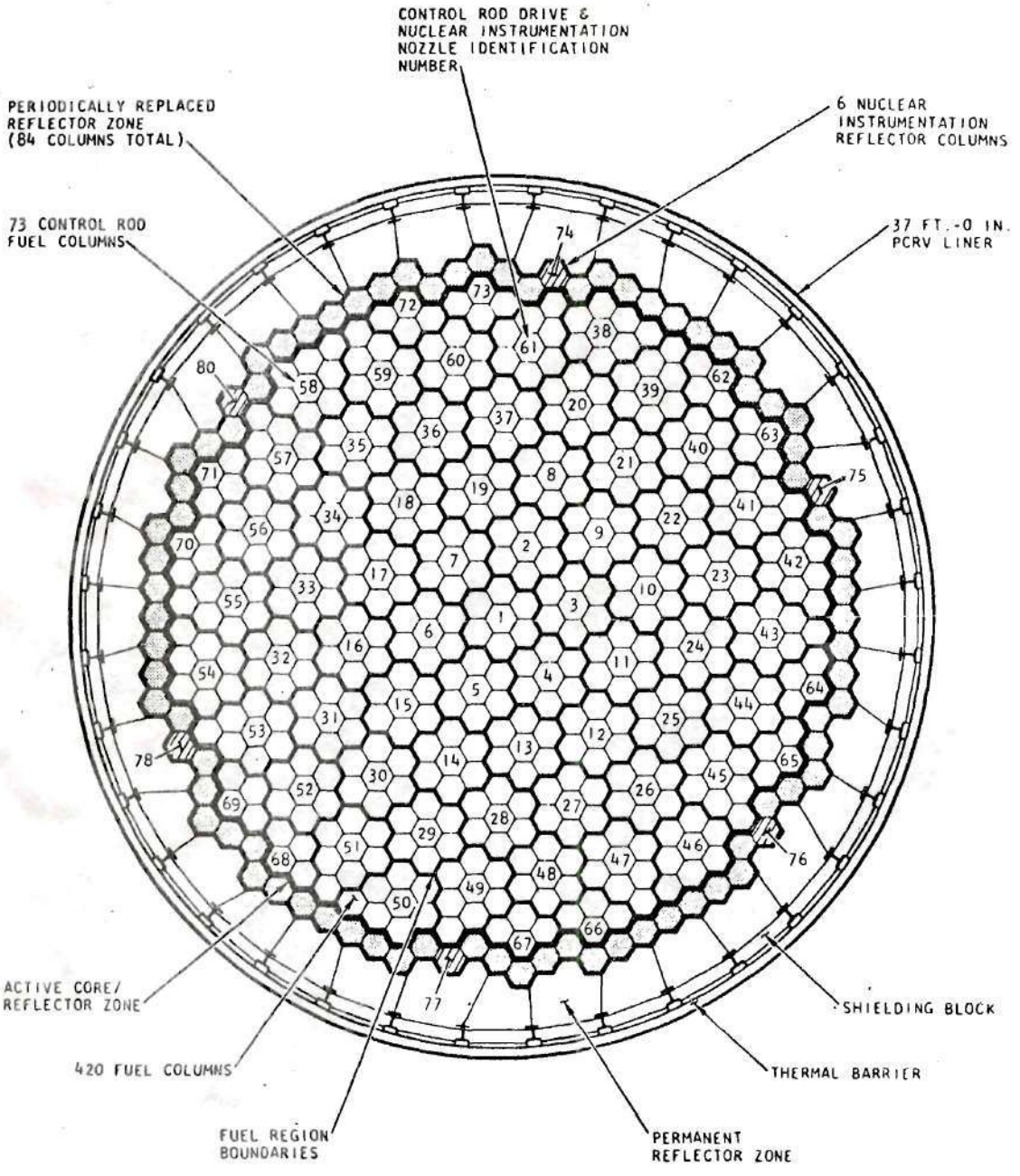

Figure 2. Plan View of Core and Side Reflector

Table 1. HTGR Parameters

Core Arrangements	
Pitch of fuel columns within refueling region, in.	14.21
Number of fuel columns	475
Number of hexagonal side reflector columns	96
Number of large side reflector block columns	36
Number of spacer block columns	36
Number of control rod channels	146 (2 per fuel region)
Number of reserve shutdown channels	73 (1 per fuel region)
Number of fuel regions	73
Effective active core diameter, ft	27.15
Active core height, ft	20.8
Equivalent side reflector thickness, including spacers, in.	53
Top and bottom reflector thickness, each, in.	46.83
Thermal and Hydraulic Parameters	
Total core thermal power, MW	3000
Total core helium flow, lb/hr	7.17×10^6
Coolant core inlet temperature, °F	650
Average coolant core outlet temperature, °F	1800
Coolant pressure, psia	700

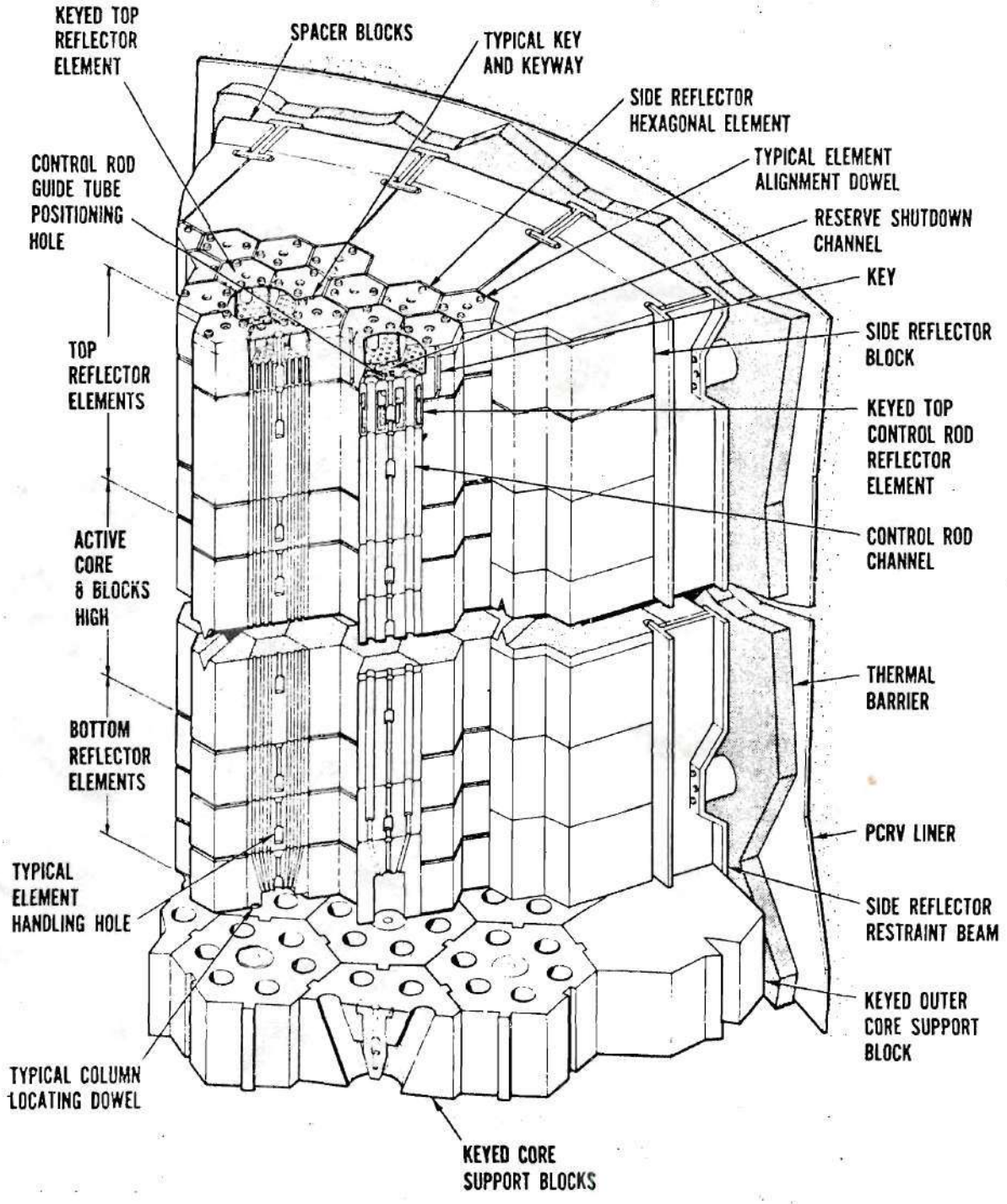

Figure 3. Elevation Section of Core Arrangement

ThC_2, varying from 0.2 to 0.4 mm in diameter, and surrounded by layers of protective coatings. ThC_2 particles are coated with BISO coatings, and UC_2 particles are protected with TRISO coatings. BISO coatings contain coating layers of two materials: a buffer layer of porous pyrolytic carbon and an outer layer of high density isotropic pyrolytic carbon. TRISO coated particles contain the buffer layer, a layer of silicon carbide, and both inner and outer layers of high density isotropic carbon. The more protective TRISO coatings are used for the UC_2 particles, as these particles sustain a higher burnup. In both particles, the buffer layer permits expansion of the fuel kernel to occur during fuel residence time, and also provides a porous structure that accommodates gaseous fission products generated in the fuel kernel. The outer layer of dense isotropic carbon gives structural stability to the fuel pellet and also serves as a final barrier to the release of fission products. For the TRISO particles, the silicon carbide coating provides for the retention of metallic fission products.

It is possible to vary the isotopic composition of the fissile fuel particles, the ratio of fissile to fertile fuel particles, and the ratio of fuel particles to carbon in the fuel rod. The primary purpose of this project is to optimize these variables for an equilibrium fuel cycle. The approach to equilibrium and the specific fuel compositions for a fuel scheme are discussed later.

Fuel Rods

The fuel composition is controlled by the number of fissile fuel particles and fertile fuel particles that are specified for each fuel rod.

The specified number of fertile and fissile particles are mixed homogeneously in a carbon "glue," and bonded into cylindrical fuel rods. The rods have a diameter of about 0.625 inches, and a length of about 2 inches. A stack of 15 such small rods fills one fuel hole in a fuel element. The fuel composition of the fresh fuel rods may vary with axial and/or radial position in the core. This will be discussed in Chapter II.

Fuel Elements (Standard and Control)

The fuel rods are grouped into fuel elements, which are the basic units of the core fuel system. There are 3800 individual fuel elements in the core of the particular design considered. They are hexagonal in cross section, 14.17 inches across flats and 31.22 inches high. The fuel rods are contained in an array of 0.631 inch diameter fuel holes that are parallel with the coolant channels and occupy alternating positions in a triangular array within the graphite structure of the fuel element. The fuel element structural (and moderator) material is conventional nuclear grade needle-coke graphite. The fuel holes are drilled from the top face of the fuel element to within about 0.3 inches of the bottom face. Standard fuel elements are those without control rod channels; these typically contain 132 fuel rods and 72 coolant channels. Figure 4 shows a standard fuel element.

Approximately one out of every seven fuel elements contains channels for control rods and reserve shutdown absorber material, as shown in Figure 5. Except for the two control rod channels and the reserve shutdown hole, the control fuel element is like the standard fuel element. Each control fuel element contains 76 fuel rods and 43 coolant channels.

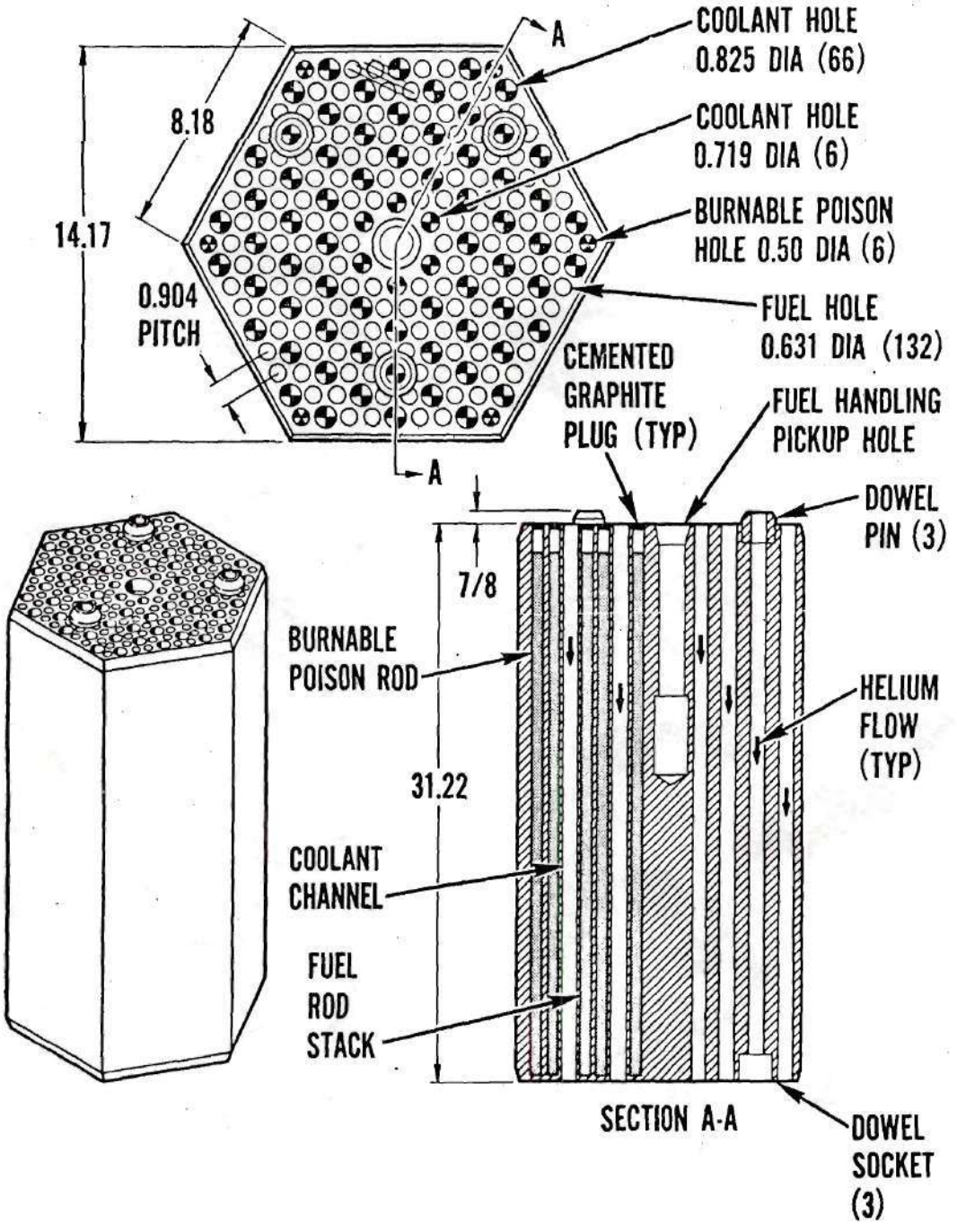

Figure 4. Standard Fuel Element

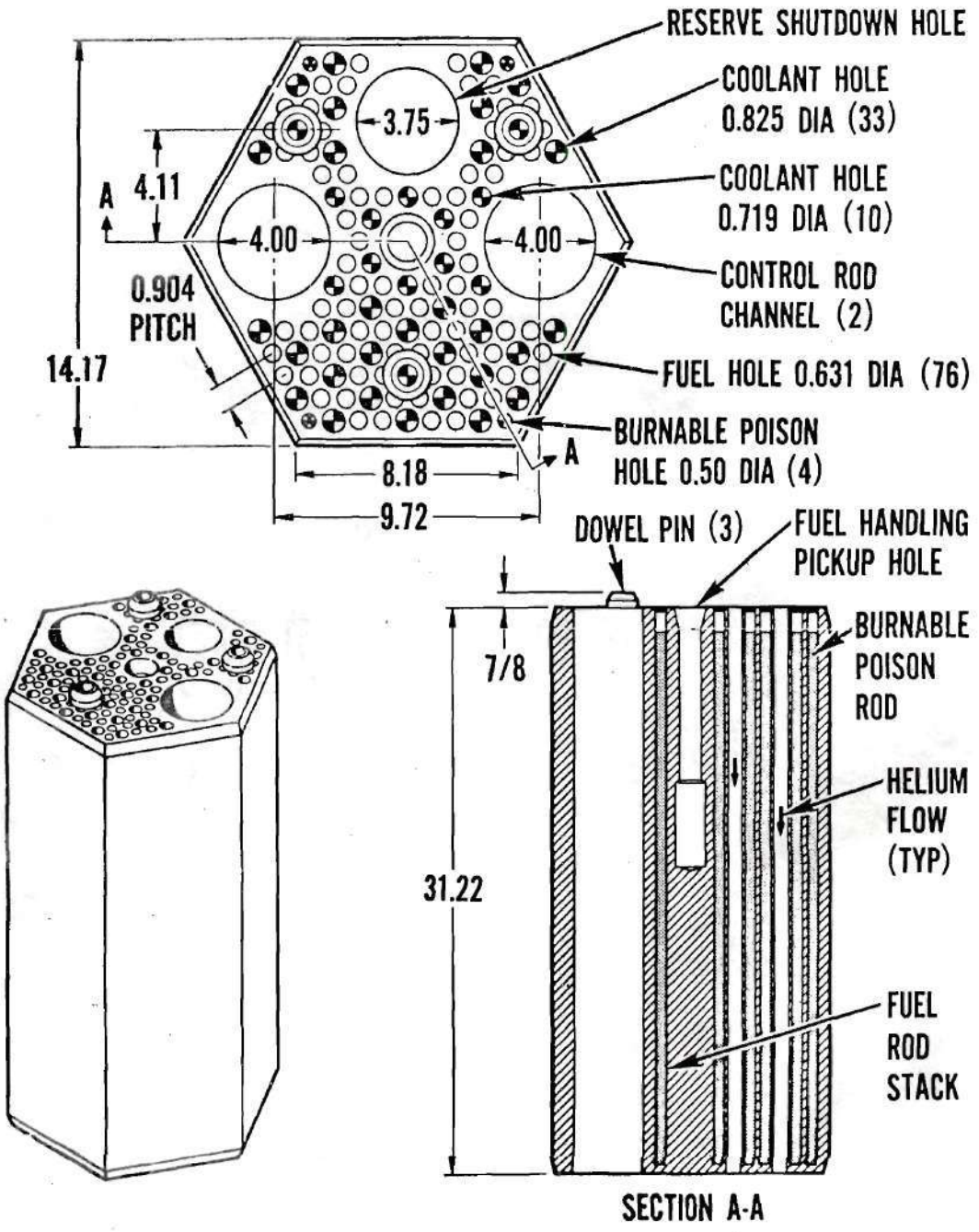

Figure 5. Control Fuel Element

Figures 4 and 5 show that both the standard fuel element and the control fuel element have burnable poison holes at the perimeter of the fuel element. A burnable poison is a neutron absorber which is depleted through core exposure. In the HTGR the poison is in the form of boronated-graphite rods, 0.5 inches (or less) in diameter, running the length of the axial column. The presence of a burnable poison is most important at the beginning of the fuel cycle, as it serves to hold down the initial excess reactivity of the core. Both the poison and the fuel are simultaneously depleted during core exposure; however, the poison is depleted at a faster rate. This tends to stabilize the reactor power shape and minimize the use of control rods. The amount of burnable poison present in the fuel elements is an important variable in this investigation.

Fuel Columns

A fuel column is a stacked arrangement of eight fuel elements, which are either all standard or all control fuel elements. The fuel elements are aligned in the axial direction by three graphite dowels which are located on the top face of each fuel element. The dowels are used to secure the fuel element to those above and below it. They also insure the proper alignment of coolant channels, control rod channels, and the reserve shutdown hole, along the entire axial length of the column. There are 475 fuel columns in the core of the 1100 MW(e) design.

Fuel Regions

Typically the standard and control fuel columns are grouped into "regions" (or "patches") consisting of a central control fuel element column surrounded by six standard fuel element columns. There are 73 fuel regions, although some of the perimeter regions contain only four fuel

columns. The regions are outlined in Figure 2. Surrounding the fuel regions are replaceable and permanent side reflectors mainly composed of graphite and a boronated absorber. In the axial direction, each fuel region is made up of eight layers of fuel elements in addition to top and bottom reflector zones. Thus, a typical region contains eight control fuel elements in the central axial column position and 48 standard fuel elements in the six surrounding fuel columns.

The 73 pairs of control rods (one pair per region) consist of boron carbide in a graphite matrix and sheathed in stainless steel cans. The two control rods in each region are inserted and withdrawn together; the average worth of a rod pair is about 0.0004 Δk. The control rods are used both as shim rods for power shaping and to shut down the reactor; their role in power shaping will be discussed in Chapter III. The reserve shutdown system utilizes boronated graphite balls to provide backup shutdown capability. The balls are stored in a hopper within each control rod drive assembly and are released into the reserve shutdown channel if required. In the absence of control rods the reserve shutdown system is sufficient by itself to shut the hot operating reactor down to refueling temperature.

CHAPTER II

FUEL SHUFFLING SCHEMES FOR THE HTGR

This chapter will discuss two separate methods by which fuel can be arranged in the core of the proposed HTGR. In both cases, fuel age (in-core residence time) and fuel composition determine the placement of the individual fuel elements. The fuel elements are arranged at each yearly reload such that the fuel placement pattern for each yearly fuel cycle is nearly the same. One-fourth of the fuel elements are reloaded annually. In a radial fuel loading scheme, fresh fuel is added at designated radial positions as entire axial fuel columns, and fuel columns with four-year residence time are removed from the core. In an axial fuel shuffling scheme, fresh fuel elements are added at designated axial positions for every fuel column. Aged fuel is shuffled to a new axial position in the fuel column, and four-year old fuel is removed.

Radial Fuel Loading[5]

Radial fuel loading schemes are widely used for light water reactors, and a radial scheme could be used for the HTGR. One of the features of this scheme is that each fuel element in a given axial fuel column has the same age, whereas for an axial fuel shuffle scheme this is not the case. In a radial loading scheme, the fuel columns with differing age are distributed throughout the core in a pattern that is designed to yield a radial power distribution that is as flat as possible.

The radial fuel loading scheme can utilize "zoning" in both the axial and radial directions to shape the power distribution and thus flatten fuel temperatures. A zone is a ring of adjacent fuel regions of varying age. Within a zone, fuel elements of a given age initially have nearly the same composition. Fuel regions of the same age, yet in different zones, have different initial compositions. The radial zoning scheme can be illustrated with reference to Figure 6. Figure 6 shows five zones of different fuel compositions, which were chosen to yield a relatively flat radial power distribution. The five zones are defined as follows:

Zone 1: Radial fuel region 1

Zone 2: The six fuel regions surrounding Zone 1

Zone 3: The 12 fuel regions surrounding Zone 2

Zone 4: The 54 fuel regions surrounding Zone 3, excluding fuel columns adjacent to the radial reflectors

Zone 5: The ring of fuel columns adjacent to the radial reflectors

Zone boundaries coincide with fuel region boundaries except for Zone 5. Those regions of a given zone which are the same age contain the same fuel and burnable poison loads. With proper fuel compositions, this loading pattern is designed to yield a maximum "radial peaking factor" of 1.6. That is, the maximum power produced in any fuel region will be 1.6 times the average region power production.

In the radial fuel loading scheme, there are two main features which tend to flatten the radial power distribution. The fuel toward the core periphery (especially Zone 4) tends to be heavily loaded with uranium. This tends to prevent a power peak at the center of the core which would

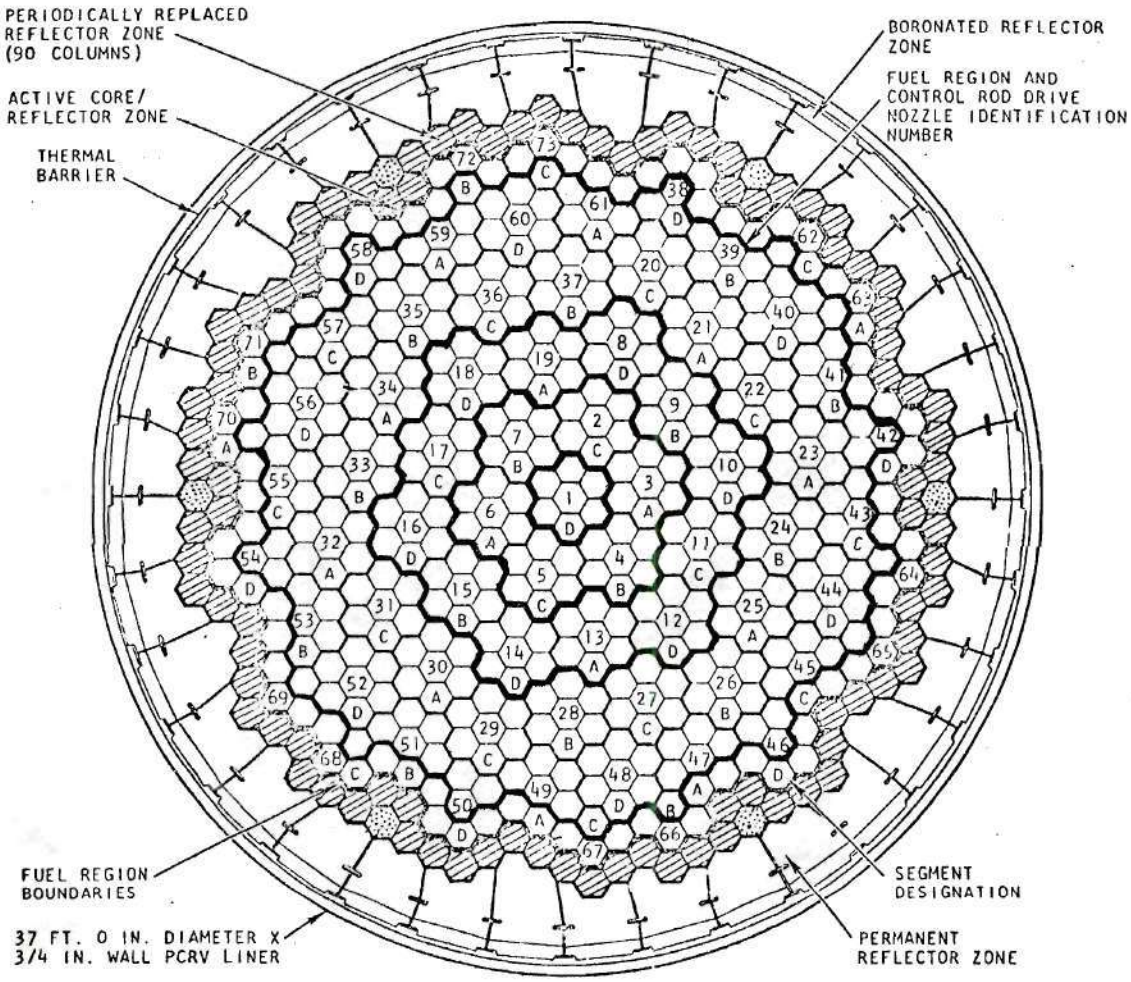

FOR THE INITIAL CORE:

"3 YEAR OLD" FUEL SEGMENT I.D. = A
"2 YEAR OLD" FUEL SEGMENT I.D. = B
"1 YEAR OLD" FUEL SEGMENT I.D. = C
"0 YEAR OLD" FUEL SEGMENT I.D. = D

Figure 6. Core Configuration; Region and Segment Identification

otherwise have occurred for a more homogeneously loaded core. Secondly, the ring of elements adjacent to the outer reflector, Zone 5, is heavy in thorium and moderate in uranium to minimize power peaking at the core-reflector interface. Considerable "reflector peaking" would otherwise result from in-leakage of predominantly thermalized neutrons from the reflector.

Axial zoning is also utilized to provide varying fuel compositions such that the resulting axial power distribution will be tilted toward the core inlet (top of core). It is desired that even in the presence of partially inserted control rods, the power fraction in the top half of the core should still be 50 percent or more. The motivation for a top-peaked axial power distribution is discussed in the next section. In a proposed scheme, fuel is zoned axially into three zones. The top zone is most heavily loaded in both thorium (1.20 times average axial concentration) and uranium (1.23 times average axial concentration). The bottom zone has the lightest fuel load.

Axial Fuel Shuffling

In the radial loading scheme, the fresh fuel is put into the core as entire axial columns of fuel elements, and they remain together in the same relative axial positions until they are removed after four years of core exposure. In axial fuel shuffling, fresh fuel is added yearly to a specified axial position in each fuel column, each other fuel element in the column is moved to a new axial position, and four-year old fuel is removed from each column. Each fuel column is identical with respect to the fuel elements' age and axial position. With axial shuffle, as with radial

loading, the radial power distribution is flattened by radial zoning (i.e., fuel composition variations in the radial direction). The axial power distribution is shaped by the axial shuffling pattern.

The main advantage of an axial fuel shuffling scheme is that it can be used to reduce the peak radial power level, or radial peaking factor. This can result in a higher average outlet gas temperature. As was mentioned, a proposed radial fuel loading scheme results in a maximum radial peaking factor of about 1.6. The peak radial power levels typically occur in the fuel columns which contain fresh fuel, and in the regions which are most heavily fueled. This is not a problem in the axial shuffle scheme, as all fuel columns are equally aged. For an axial fuel shuffle scheme with radial zoning, a radial peaking factor as low as 1.2 can be achieved. Thus the ratio of maximum-to-average radial power production is reduced by 25 percent through use of axial fuel shuffle. This is important because it also reduces the ratio of maximum-to-average radial fuel temperature. The peak fuel temperature is restricted by material limitations. With the flattened temperature profile associated with axial fuel shuffle, the average fuel temperature will be higher when the peak fuel temperature is at the limiting value. Because of this, the average outlet gas temperature can be increased; this is especially important for process heat applications. It should be noted that the primary motivation for using axial fuel shuffling is that it allows a higher average outlet gas temperature than does radial fuel loading. Thus, it is possible to generate more power with the axial fuel shuffling scheme, without violating the fuel temperature limitations.

A disadvantage of axial fuel shuffle is that each fuel element must be handled at each reloading. Also, it is difficult to establish an axial shuffle pattern which yields an acceptable axial power distribution throughout life. The optimum axial power distribution will be discussed next.

Optimum Axial Power Distribution

In the radial direction the optimum power distribution is flat, or equivalently, it represents a 1.0 radial peaking factor. This results in an equal outlet gas temperature for each radial fuel region, if axial power distributions are identical for all regions. With the optimum axial power distribution, all the fuel would operate at a maximum temperature which is determined by fuel material limitations. This would result in the maximum allowable outlet gas temperature in each radial fuel region. In the axial direction the optimum power distribution is exponential, as will be shown, with the maximum power levels at the core inlet (top). The optimum power distribution is that which allows a maximum average outlet gas temperature while limiting fuel temperatures to a value specified by material limitations.

The typical arrangement of fuel rods and coolant channels in the radial direction is shown in Figure 4. With this pattern, the ratio of fuel rods to coolant channels is two-to-one; or the equivalent of two fuel rods supply heat to each coolant channel.

Heat transfer from a fuel rod to a one phase coolant may be expressed by the following energy equations. (Nomenclature is given in Table 2.)

Table 2. Nomenclature

A	total surface area for heat transfer in one coolant channel, ft^2
B	MC_p/UA, heat transfer parameter, dimensionless
C_p	heat capacity of coolant, Btu/lb - °F
H	thermal power output for one coolant channel, Btu/hr
L	fuel channel length, ft
M	coolant mass flow rate, lb/hr
p(z)	normalized axial power distribution, dimensionless
q(z)	axial power distribution, Btu/hr/ft of element
t(z)	$(T_s-T_o)/\Delta T$, normalized axial center-line fuel temperature, dimensionless
t_m	optimum t(z) (a constant), dimensionless
$T_c(z)$	bulk coolant temperature, °F
T_o	coolant inlet temperature, °F
$T_s(z)$	axial center-line fuel temperature, °F
U	overall heat transfer coefficient (conduction and convection) from $T_s(z)$ to $T_c(z)$, Btu/hr-ft^2-°F
z	axial distance, ft

$$q(z) = MC_p \frac{dT_c(z)}{dz} \tag{1}$$

also
$$q(z) = \frac{UA}{L}\left(T_s(z) - T_c(z)\right) \tag{2}$$

Note that U is the overall heat transfer coefficient (conduction and convection) from the center-line fuel temperature (T_s) to the bulk coolant temperature (T_c), for the configuration shown in Figure 4. It is assumed that U and C_p are independent of both temperature and axial position (z), and that U does not change with fuel burnup.

By integrating (1) and substituting into (2) for T_c, the solution for T_s is:

$$T_s(z) = T_o + \frac{\int_o^z q(z)dz}{MC_p} + \frac{q(z)}{\frac{UA}{L}} \tag{3}$$

The following variables are introduced:

$$\Delta T = \frac{H}{MC_p} = \text{gas temperature rise in the coolant channel}$$

$$t(z) = \frac{T_s(z) - T_o}{\Delta T} = \text{normalized axial temperature}$$

$$B = \frac{MC_p}{UA} = \text{dimensionless heat transfer parameter}$$

$$p(z) = \frac{q(z)}{\frac{H}{L}} = \text{normalized axial power distribution}$$

such that:

$$\frac{1}{L}\int_{o}^{L} p(z)dz = 1$$

Note that p(z) is the power density at axial position z, divided by the average axial power density.

Equation (3) becomes:

$$t(z) = \frac{1}{L}\int_{o}^{z} p(z)dz + Bp(z) \qquad (4)$$

Equation (4) relates the normalized center-line fuel temperature distribution, t(z), to the normalized axial power distribution, p(z), and the dimensionless heat transfer parameter, B (which is assumed to be independent of t(z) and z).

The optimum axial power distribution is that which gives a constant center-line fuel temperature, t_m, at each point along the axial length of the fuel rod. With such a power distribution, the average outlet gas temperature will be maximized for a given fuel material temperature limit. Thus, the optimum p(z) will make $t(z) = t_m$ = a constant.

$$t(z) = t_m = \frac{1}{L}\int_{o}^{z} p(z)dz + Bp(z) \qquad (5)$$

Differentiating:

$$0 = \frac{1}{L}\, p(z) + B\,\frac{dp}{dz}$$

The solution is:

$$p(z) = \frac{e^{-\frac{z}{LB}}}{k} \quad (k \text{ is a constant}) \tag{6}$$

with the condition:

$$\frac{1}{L}\int_0^L p(z)dz = 1 \tag{7}$$

Substituting (6) into (7), it is found:

$$k = B\left(1 - e^{-\frac{1}{B}}\right) \tag{8}$$

The final solution is:

$$p(z) = \frac{e^{-\frac{z}{LB}}}{B\left(1 - e^{-\frac{1}{B}}\right)}$$

The value of B is determined by the heat transfer characteristics of the fuel and the helium coolant. For the HTGR applicable to process heat applications, the optimum axial power distribution is:

$$p(z) = 2.26\ e^{-1.955\left(\frac{z}{L}\right)}$$

This power distribution is shown in Figure 7.

As p(z) is defined, it is equal to the axial power density at point z divided by the average axial power density. This is also called the "axial peaking factor." The ideal power distribution for this HTGR would have a maximum axial peaking factor of 2.26, at the top of the core (z = 0). It would have a minimum axial peaking factor of 0.32 at the bottom of the core (z = L).

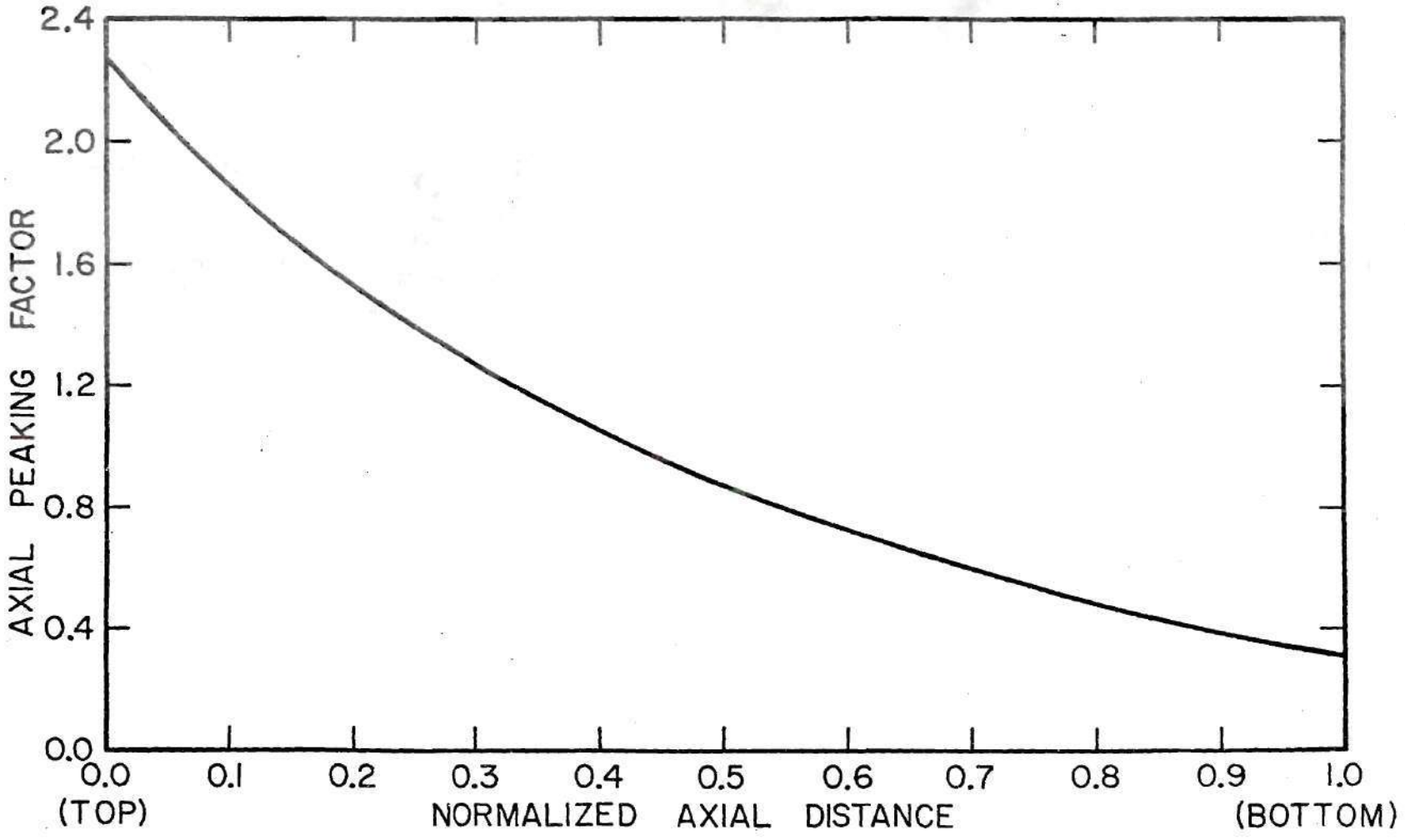

Figure 7. Ideal Axial Power Distribution for HTGR

In this project several axial push through fuel schemes were investigated, in an attempt to approximate the above axial power distribution. The axial push through scheme was described in Chapter I. In this scheme the fuel age increases from the top to the bottom of the core, and the fuel concentration decreases from top to bottom. This scheme naturally results in power distributions peaked at the top of the core. The problem is to establish correctly shaped power distributions without prohibitively high peak power levels throughout the fuel lifetime.

Equilibrium Versus Initial Fuel Cycles

A reactor fuel cycle is in equilibrium when the same fresh fuel load is added to the core yearly, and the same depleted fuel load is removed yearly. In this project, consideration was given to fuel cycles which approximate "recycle" equilibrium conditions. Under recycle conditions, U^{233} (which is bred from Th^{232}) is included in the fresh fuel load. The initial core, however, will only be fueled with thorium and "fresh feed" uranium. Fresh feed uranium, from an enrichment plant, contains:

1.03 % U^{234}

92.63 % U^{235}

0.23 % U^{236}

6.11 % U^{238}

As the fresh feed uranium contains no U^{233}, it would be impossible for the initial core to match the expected recycle equilibrium core composition. It would also be difficult and costly to try to match the various partially depleted fuel elements of the equilibrium cycle with varied concentrations of fresh feed fuel. As a consequence, the initial fuel cycle and the first

several reloads are poor approximations to an equilibrium cycle. With each reload, however, equilibrium conditions should be more closely approximated.

It is estimated that it will take about five years of reactor operation for the fuel cycle to approximate a first nonrecycle equilibrium. During the nonrecycle equilibrium there is no bred U^{233} in the fresh fuel load, as there is during recycle equilibrium. During the first five years of core life, the fresh fuel added yearly will be composed of fresh feed uranium and thorium. At the end of this period, bred U^{233} will be recycled and used as a fissile material in the reload segments, with fresh feed uranium added as makeup fuel as required. This assumes that the necessary facilities are available for processing U^{233}. With the addition of U^{233}, an approach to the final recycle equilibrium begins. It is expected to take five years before this recycle equilibrium is approximated.

CHAPTER III

AXIAL PUSH THROUGH FUEL SCHEME INVESTIGATIONS

Criteria for Optimum Fuel Scheme

The criterion assumed herein on the fuel temperature limit was that the maximum fuel temperature should not exceed 2850°F during normal full-power operation. To operate at the specified power level, the axial temperature profile must be nearly flat in order to satisfy this requirement. This requirement must be satisfied at all times during the yearly cycle, from immediately after reload when the core is heavily fueled, until the end of the cycle when control rods are nearly withdrawn from the core.

In order to satisfy this requirement, and obtain a maximum outlet gas temperature, the axial power distribution should approximate the ideal exponential shape with peak power levels at the core inlet. The desired power distribution must also be stable to both control rod movement and fuel burnup; i.e., it must be relatively invariant under these changes. Also, the K_{eff} values of the control-rodded core should change by only a small amount throughout fuel burnup to insure that the reactor can be easily controlled. The control rods will be gradually withdrawn during the year to compensate for fuel depletion. It has been determined[6] that the freshly-fueled core can be controlled by 13 or fewer control rod pairs inserted into their fuel regions. By the end of the year, these rods would be nearly withdrawn in an optimum fuel scheme. Complete withdrawal would insure maximum burnup of the fuel.

For an optimum fuel scheme, the radial power distribution is flat. In an axial fuel shuffle scheme, the radial power distribution is controlled by the radial zoning pattern. The investigations which are described next attempt to optimize the fuel scheme in the axial direction only. Radial zoning is not considered. However, the thermal analysis which is discussed later does consider the radial power distribution.

Initial Fuel Cycle Investigations

An axial push through fuel scheme was the only fuel shuffle pattern considered in this project. This scheme was described in Chapter I. The purpose of the initial axial push through fuel scheme investigations was to find the fuel concentrations which would establish an acceptable axial power distribution. The initial investigations were for supercritical unrodded cores (no control rods inserted). The nuclide concentrations of uranium (fresh feed uranium plus recycled U^{233}), thorium, and the burnable poison B^{10} were the variables in these investigations. When acceptable power distributions were obtained, the behavior of the control rodded core was investigated. The fuel cycles were investigated by using a one-dimensional fuel depletion code, FEVER, which will be discussed next.

FEVER

FEVER is a one-dimensional neutron diffusion-depletion program which calculates the spatial distribution of the neutron flux, the effective multiplication factor (K_{eff}), the spatial composition, and the spatial power distribution of a radial fuel region for a period of time and for the reactor operating conditions specified by the user. In these investigations, all of these quantities were calculated in the axial direction;

a cylindrical geometry was used, and all parameters were constant in the radial direction (the radial flux is nearly flat across a single fuel region). These quantities were calculated using a one-dimensional diffusion theory routine which allows up to 100 mesh intervals, spaced uniformly in each of a maximum of 20 spatial regions. In these investigations, 11 axial regions (two top reflector regions, eight fuel regions, and a bottom reflector region) were divided into 92 mesh intervals. The axial regions used in the FEVER investigations represented the homogenized layers of a typical fuel region. The typical fuel region contains six standard fuel element columns and a central control fuel element column.

Seven neutron energy groups were used, with both upscatter and downscatter as specified by the nuclide cross section blocks. Seven-group cross section information was given for each nuclide. This included: the fission, n-2n, capture, transport, and group-to-group transfer microscopic cross sections.

In these investigations, a nuclide depletion scheme was used which consisted of 36 nuclides: the five uranium isotopes, thorium^{232}, seven daughter nuclides resulting from the fuel, twenty fission products, the burnable poison boron^{10}, carbon, and a "nuclide" representing the boron carbide control rods. The number densities of each of these nuclides were specified for each axial region. Depletion of the nuclides is calculated separately for each axial region, assuming exposure to the average group-dependent flux of that region. The depletion calculations are made at time intervals specified by the user. In these investigations, depletion calculations were made 30 times during the fuel cycle year, and complete

outputs including K_{eff} values and axial power distributions were printed at 10 time points during the fuel cycle year. The depletion calculations can be interrupted at any time, so that fuel can be added to any region, moved to another region, or removed from the reactor. In the initial investigations there were three such reloads, each at yearly intervals. During the reload, fuel was shuffled according to the axial push through shuffling scheme. Thus, the fresh fuel in the initial core was moved to the bottom of the core, and was ready to be removed at the end of the third reload year. The total core residence time of the discharged fuel was four years.

Basically, FEVER solves two groups of coupled equations. These are the nuclear burnup equations and the multigroup neutron diffusion equations. The nuclear burnup equations are solved, in each region separately, for the nuclide concentrations as a function of burnup time. The initial regionwise nuclide concentrations are specified by the user. The burnup equations calculate the change in nuclide concentrations during the burnup period. The nuclide concentrations can be increased by the decay of a precursor, and by fission, n-2n reaction, or neutron capture in another nuclide. The nuclide concentrations can be decreased by these same mechanisms. In both cases, an average energy-dependent flux is used in each region.

Numerically, the change in a region's nuclide density, x_i, is expressed as:

$$\frac{dx_i}{dt} = - d_{ii}x_i + \sum_{\substack{j=1 \\ j\neq i}}^{N_x} d_{ij}X_j, \qquad i = 1,2,\ldots N_x$$

where, for each region, d_{ii} is a depletion term and d_{ij} is a production term.

$$d_{ii} = \sum_{g=1}^{G} (\sigma_c^g + \sigma_f^g + \sigma_{n-2n}^g)_i \, \bar{\phi}_{r,g} + \lambda_{ji}$$

$$d_{ij} = \sum_{g=1}^{G} (\sigma_{c_{ij}}^g + \sigma_{n-2n_{ij}}^g + \Gamma_{ij} \, \sigma_{f_j}^g) \, \bar{\phi}_{r,g} + \lambda_{ij}$$

where: i = nuclide index

r = index of the region where burnup takes place

g = energy group index

N_x = number of nuclides in depletion scheme

ij = nuclide subscripts; the one appearing first represents the daughter product, and the second subscript indicates the parent nuclide

G = number of energy groups

$\bar{\phi}$ = average neutron flux

Γ_{ij} = fission yield of a fission product i from a fissionable nuclide j

λ = disintegration constant

σ_{n-2n} = effective microscopic total n,2n cross section (shielded)

σ_f = effective microscopic fission cross section (shielded)

σ_c = effective microscopic capture cross section (shielded)

t = time

The average energy-dependent fluxes for each region are found as a solution to a one-dimensional multigroup neutron diffusion equation. The

macroscopic cross sections used in this equation utilize the regionwise number densities from the solution to the burnup equation. The boundary conditions used in the diffusion equation are specified by the user. In these investigations zero-current, or "infinite core," boundary conditions were used.

Unrodded Trials and Results

There are two major differences between these initial unrodded investigations and the final control-rodded investigations. Without control rods, the K_{eff} values of the initial investigations should obviously be greater than unity throughout the cycle year (between about 1.05 and 1.01). With control rods, the K_{eff} values should ideally be unity. Calculationally, they decrease from slightly above unity to slightly below unity (e.g., 1.01 to 0.995) during the burnup period. Secondly, the first trials of the unrodded fuel schemes will be far from equilibrium cycles. When a new fresh fuel is investigated, the nuclide concentrations of the aged fuels are not known. Instead, concentrations of aged fuels in similar fuel cycles are used as a first approximation. Often it takes up to six reloads to approximate the new equilibrium cycle. This was especially true in the first trial.

The first trial used the following nuclide concentrations in both fresh fuel regions (the top two fuel regions in the core).

TRIAL 1: Fresh Fuel Concentrations (In units of 10^{24} $\frac{\text{atoms}}{\text{cm}^3}$)

Th^{232}	33.550×10^{-5}
U^{233}	0.596×10^{-5}
U^{234}	0.327×10^{-5}

U^{235}	1.190×10^{-5}
U^{236}	0.132×10^{-5}
U^{238}	0.072×10^{-5}
B^{10}	0.035×10^{-5}
C	6710.000×10^{-5}

This fresh fuel load has a carbon-to-thorium ratio of 200, and a carbon-to-uranium ratio of 2880. The uranium composition represents about 35 percent recycled U^{233}, and 65 percent fresh feed uranium. After six reloads, this fuel cycle approximated equilibrium conditions reasonably well; for example, the concentration of the discharged U^{235} differs by less than one percent at the last two reloads.

At equilibrium, the power distributions were good approximations of the desired exponential shape. However, the K_{eff} values were unacceptable, as the end-of-cycle (EOC) values dropped to 0.964. In all of the initial unrodded trials, FEVER output was obtained at ten time points during the fuel year. These were: initial core (t = -1), two days later--after the buildup of Xe^{135} (t = 0), and at the end of eight time steps of 36.525 days each (t = 1 through 8). This makes a total of 292.2 days of full-power operation, which is used to represent one full year of operation at 80 percent full power. The maximum total-core K_{eff} values which occurred during each of these periods, for this first trial, are listed in Table 3.

In order to raise the EOC K_{eff} values, more uranium was used in the fresh fuel for Trial 2. The isotopic uranium ratios remained the same, but 11 percent more uranium was used. Also, the burnable poison

Table 3. Results from Trials 1 and 2

Time Step	Days	Trial 1 Max. K_{eff}	Trial 2 Max. K_{eff}
-1	0	1.0665	1.0415
0	2	1.0348	1.0146
1	37	1.0189	1.0105
2	73	1.0132	1.0163
3	110	1.0049	1.00183
4	146	0.9964	1.00150
5	183	0.9875	1.0082
6	219	0.9793	1.0000
7	256	0.9712	0.9915
8	292	0.9640	0.9832

concentration was doubled. It was hoped that this would hold down the beginning-of-cycle (BOC) K_{eff} values, which would otherwise have increased because of an increased uranium load, but would not seriously reduce the EOC K_{eff} values. The burnable poison is reduced by about a factor of 200 during the year, while the uranium is reduced by only a factor of 0.5. Thus, the effect of the burnable poison is not nearly as important after the first few time steps. These changes did improve the K_{eff} values, but not enough to raise the EOC values to above unity, as seen in Table 3.

In Trial 2, there was a severe depression in the power distribution in the first fuel region during the first three time steps. This was due to the large amount of B^{10} present there. During these periods, the power distribution did not approximate an exponential. In Trial 3, the B^{10} was removed entirely from the top fuel region, but left unchanged in the second fresh fuel region. This succeeded in restoring a more nearly exponential power distribution at BOC. As expected, the low EOC K_{eff} values were not significantly changed.

In Trial 4, the uranium fuel concentration in the fresh fuel was again increased, by 12 percent, in an attempt to raise the EOC K_{eff} values. This objective was accomplished, but the BOC K_{eff} values were also raised considerably, as shown in Table 4. It was desired to limit the BOC ($t = 0$) K_{eff} values to about 1.05 for these unrodded trials. The increased uranium concentration also resulted in a power distribution which was too steeply peaked at the top of the core at BOC. The BOC ($t = 0$) maximum axial peaking factor was 4.52 for this trial; it occurred at the top of the core. As shown in Chapter II, the maximum axial peaking factor

Table 4. Results from Trials 4, 6, 7, and 8

Time Step	Trial 4		Trial 6		Trial 7		Trial 8	
	Max. K_{eff}	Max. Axial Peaking Factor	Max. K_{eff}	Max. Axial Peaking Factor	Max. K_{eff}	Max. Axial Peaking Factor	Max. K_{eff}	Max. Axial Peaking Factor
-1	1.1460	4.91	1.0749	3.34	1.0797	2.84	1.0701	2.68
0	1.1070	4.52	1.0442	2.81	1.0501	2.48	1.0420	2.26
1	1.0679	2.59	1.0297	1.88	1.0398	2.10	1.0342	2.02
2	1.0610	2.62	1.0291	2.26	1.0396	2.27	1.0352	2.23
3	1.0522	2.22	1.0248	1.88	1.0367	2.12	1.0343	2.12
4	1.0452	2.21	1.0227	2.02	1.0331	2.08	1.0324	2.09
5	1.0365	2.07	1.0173	1.77	1.0275	1.97	1.0281	1.96
6	1.0285	2.01	1.0134	1.86	1.0216	1.93	1.0230	1.93
7	1.0201	1.88	1.0072	1.67	1.0151	1.83	1.0169	1.85
8	1.0125	1.82	1.0029	1.77	1.0088	1.78	1.0108	1.80

for the optimum axial power distribution is 2.26. The K_{eff} values and power distribution at time step t = -1 are not of much importance, as this represents only a two day period prior to Xe^{135} buildup. During this period, control rods will be used to compensate for the absence of Xe^{135}.

In Trial 5, the concentration of Th^{232} in the fresh fuel was increased by 12.5 percent, in an attempt to lower both the BOC K_{eff} values and the BOC peak power levels. With this increase in concentration, Th^{232} accounted for more than 50 percent of the total fast absorptions in Trial 5. This absorption leads to the production of fissile U^{233}. The result of an increase in the amount of Th^{232} should be a decrease in BOC K_{eff} values, due to absorption, and an increase in the fuel cycle "conversion ratio." This is the ratio of the number of fissile atoms produced to the number of fissile atoms consumed during a given time period. Because of the increased conversion ratio, the aged fuel should be more heavily fueled relative to the fresh fuel, when the Th^{232} concentration is increased. This would result in a decreased maximum axial peaking factor in the fresh fuel. These three features were observed. The conversion ratio was increased from 0.748 at EOC-Trial 4, to 0.792 at EOC-Trial 5. The BOC (t = 0) maximum axial peaking factor was decreased from 4.52 to 3.98, and the BOC K_{eff} values were decreased from 1.1070 to 1.0640, when the Th^{232} concentration was increased.

Although the addition of Th^{232} did decrease the BOC peak power densities, these are still too high. In an attempt to further lower them, a small amount of B^{10} was returned to the top fuel region, in Trial 6. The amount of B^{10} placed in the top region was one-third of the amount

present in the second fuel region. Both the K_{eff} values and the maximum axial peaking factors were improved (decreased) as shown in Table 4.

The fuel scheme of Trial 6 was a potentially acceptable fuel scheme and was later investigated with control rods inserted. The next two trials were for fuel schemes with the same amount of uranium in the fresh fuel as in Trial 6. It was previously found[7] that fuel cycles with as large an amount of Th^{232} as in Trial 6 (carbon-to-thorium ratio of 175) tend to be quite sensitive to the movement of an absorber (control rod or burnable poison) along the axial direction. That is, there can be a large change in the axial power distribution following a change in the position of the absorber. Because of this, the Th^{232} concentration was reduced by about 5 percent in the next two trials. In Trial 7, the B^{10} concentration was also increased in the top fuel region by 65 percent, to compensate for the decrease in neutron absorption. In Trial 8, the B^{10} concentration was further raised by 30 percent in the second fuel region. This was done to "shape" the axial power distribution. The axial power distributions for Trial 8 were especially good approximations of the desired exponential shape. At BOC (t = 0), for example, the axial peaking factors were within 10 percent of the values for the ideal power distribution at each axial position. Quantitative output for Trials 7 and 8 are shown in Table 4. Trials 7 and 8 were also investigated with control rods inserted, as described next. Many of the important features of these first eight trials are summarized in Table 5. In this table, the fuel composition parameters refer to the fresh fuel only.

Table 5. Summary of Unrodded Trials

Parameter	Trial Number								Ideal Power Shape
	1	2	3	4	5	6	7	8	
Carbon/Thorium	200	200	200	200	175	175	185	185	---
Carbon/Uranium	2880	2620	2620	2180	2180	2180	2180	2180	---
B^{10} Number Density ($\times 10^{-5}$) in Region 1	0.035	0.070	0.000	0.000	0.000	0.021	0.035	0.035	---
B^{10} Number Density ($\times 10^{-5}$) in Region 2	0.035	0.070	0.070	0.070	0.070	0.070	0.070	0.091	---
K_{eff} at BOC (t = 0)	1.0348	1.0146	1.0706	1.1070	1.0640	1.0442	1.0501	1.0420	---
K_{eff} at EOC (t = 8)	0.9640	0.9832	0.9745	1.0125	1.0036	1.0029	1.0088	1.0108	---
Top-of-core Axial Peaking Factor (BOC)	2.52	1.54	4.57	4.52	3.98	2.81	2.48	2.26	2.26
Bottom-of-core Axial Peaking Factor (BOC)	0.07	0.16	0.01	0.01	0.01	0.14	0.20	0.23	0.32
Top-of-core Axial Peaking Factor (EOC)	1.50	1.69	1.57	1.59	1.76	1.63	1.64	1.66	2.26
Bottom-of-core Axial Peaking Factor (EOC)	0.40	0.34	0.38	0.37	0.24	0.36	0.36	0.34	0.32

Control-Rodded Fuel Scheme Investigations

Three fuel schemes were further investigated, using the FEVER code, to determine their behavior to control-rodded operation. Control rods were inserted into the axial fuel regions, and reactor parameters were determined by the code as in the previous investigations. In this section the word "region" refers to the axial position of the fuel element along the fuel column. The control rod insertion was done in two patterns, full insertion and partial insertion.

Fully Inserted Control Rod Investigations

In the fully inserted rod investigations, a control rod was inserted into all the axial fuel regions. A control rod number density (concentration) was found such that the K_{eff} values remained near unity for a burnup period of 100 days. The K_{eff} values were slightly greater than unity at the beginning of the burnup period, and they should drop slightly below unity by the end of the burnup period. It was desired to have as small a variation about unity as possible, as this indicates a fuel scheme which can be controlled without excessive control rod movement. At the end of the first 100 day burnup period, a new control rod number density was sought which would result in K_{eff} values near unity for a second 100 day burnup period. Again, the control rod was inserted into all the axial fuel regions. This second period number density should be lower than the first period number density, as a less concentrated rod would be required to control the partially-depleted axial fuel regions. A third control rod number density was found for a final 92.2 day burnup period. These three periods, totaling 292.2 days, represent one full year of operation at 80 percent full power.

Fuel scheme Trials 6, 7, and 8 were investigated with control rods fully inserted. The control rod number densities and the resulting K_{eff} values and maximum axial peaking factors, for the first 100 day period, are shown below.

Fully Inserted Control Rod Investigations: First 100 Day Period

	Trial 6		Trial 7		Trial 8	
Initial Control Rod Number Density ($\times 10^{24}$)	8.0×10^{-5}		11.0×10^{-5}		9.0×10^{-5}	
Time Step	Days	K_{eff}	Max. Axial Peaking Factor	K_{eff}	Max. Axial Peaking Factor	K_{eff}	Max. Axial Peaking Factor
-1	0	1.0498	3.82	1.0369	3.13	1.0305	2.67
0	2	1.0192	3.29	1.0083	2.77	1.0039	2.32
1	33	1.0035	2.14	0.9973	2.22	0.9958	1.95
2	67	1.0023	2.44	0.9968	2.35	0.9959	2.12
3	100	0.9988	2.12	0.9943	2.21	0.9943	2.03

Tne only undesirable features of these power distributions were the high BOC (t = 0) maximum axial peaking factors for Trials 6 and 7. The power distributions in Trial 8 were especially good approximations of the desired exponential shape. The smallest change in K_{eff}, from time step 0 to time step 3, occurred for Trial 8 ($\Delta k = 0.0096$). Because of limited computer time, it was decided to investigate only Trial 8 further. This trial appeared most favorable with respect to both the acceptability of the power distributions and the range of the K_{eff} values.

The fuel scheme of Trial 8 was similarly investigated for eight more fully rodded burnup periods: the second and third periods of the

first fuel cycle year, the three periods of the second fuel cycle year, and the three periods of the third fuel cycle year. Listed below are the control rod number densities and the resulting initial (t = 0) and final (t = 3) K_{eff} values, for each of these periods.

Fully Inserted Rod Investigations: Trial 8 Fuel Scheme

Year	Period	Days	Control Rod Number Density ($\times 10^{24}$)	Initial K_{eff}	Final K_{eff}
1	1	100	9.0×10^{-5}	1.0039	0.9943
	2	100	8.1×10^{-5}	1.0009	0.9878
	3	92.2	5.5×10^{-5}	1.0078	0.9895
2	1	100	9.0×10^{-5}	1.0008	0.9902
	2	100	7.8×10^{-5}	0.9991	0.9849
	3	92.2	5.0×10^{-5}	1.0067	0.9879
3	1	100	9.0×10^{-5}	0.9991	0.9878
	2	100	7.5×10^{-5}	0.9991	0.9838
	3	92.2	5.0×10^{-5}	1.0033	0.9840

These figures indicate that this rodded fuel scheme is not in exact yearly equilibrium. For the equilibrium fuel scheme, the same fuel concentrations would exist for each first yearly period, each second yearly period, and each third yearly period. Thus the required control rod concentrations should not change from one year to another. By the third year, however, this rodded fuel scheme does approximate equilibrium conditions. This is indicated by the nearly identical control rod number densities, and

associated K_{eff} values, for the second and third year periods.

At each of the time periods during these three fuel cycle years, the reactor parameters were favorable. The changes in K_{eff} values were small throughout these burnup periods. For example, the K_{eff} values decreased by less than 0.02 during each period of the third year. The axial power distributions were good approximations of the desired exponential shape. However, the merit of the power distributions is best evaluated through the results of the thermal analysis code, POKE, which is discussed later.

It should be noted that this control pattern (full insertion of a control rod whose number density changes to compensate for fuel burnup) is not representative of the control pattern as it is now designed. The fully inserted control rod investigations correspond to a pattern in which several control rods would be inserted into a fuel region. During burnup, they would be individually removed from the core. This corresponds to the decrease in number density of a single fully inserted rod during burnup. As presently designed, however, the control rods in each region will be withdrawn upward to the same level in the core to compensate for fuel burnup. The only control rod number density changes are the result of neutron absorption, and these changes are small. This control rod withdrawal pattern was investigated next.

Partially Inserted Control Rod Investigations

A second set of investigations was done for a control rod withdrawal pattern which is more representative of the control rod operation as it is now designed. These investigations differ from the fully inserted control rod investigations in the manner in which the control rod is removed from

the fuel regions during burnup.

Multi-region Rod Withdrawal. In these partially inserted rod investigations, a control rod was first inserted into all the axial fuel regions, and remained there throughout the first time period (100 days). Through the first period, this investigation was nearly identical to the fully inserted rod investigations. At the beginning of the second time period, the rod was withdrawn upward to a level which allowed the K_{eff} values to remain near unity throughout the second time period (100 days). It was found that removal of the control rod from the bottom three axial fuel regions was required. That is, during the second time period the control rod number densities were set to zero in the bottom three fuel regions. The control rod number density of each region was shifted to the region three positions above, to account for the upward withdrawal of the control rod. At the end of the first burnup period, the control rod number densities had been reduced by less than 0.7 percent in any region, due to neutron absorption. Thus, the control rod number densities are virtually unchanged in the top five fuel regions for the second time period. At the end of the second time period, the control rod is again withdrawn in order that the K_{eff} values remain close to unity throughout the last time period of the fuel cycle year. It was found that a withdrawal through two more fuel regions was required. As a result, only the top three axial fuel regions contained control rods during the last time period.

In actual reactor operations, the control rods can be withdrawn at much shorter time periods, and over much shorter distances. Thus, if these investigations indicate that the reactor parameters are acceptable

under these gross rod withdrawal conditions, it is expected that the reactor parameters would be more favorable in actual operation. The most important results of these control-rodded investigations are the axial temperature profiles, which are discussed in detail later. To insure acceptable axial temperature profiles, the axial power distributions should approximate the desired exponential shape, and must be reasonably stable to the partial withdrawal of control rods. The K_{eff} values must also change by only a small amount following the partial withdrawal of control rods, to insure easy reactor control.

The nuclide number densities from the fully inserted control rod investigations were used to begin the partially inserted control rod investigations. The yearly control rod conditions and the quantitative reactor parameters which were found to exist after one year of partial rod insertion are listed in Table 6. Included in this table are the normalized axial positions where the maximum axial peaking factors occur; the top of the fuel column has a normalized position of 0.0, the bottom of the fuel column has a normalized position of 1.0.

During the first period, when the control rod is fully inserted, all the reactor parameters are favorable. The axial power distributions are all good approximations of the desired exponential shape, and all are peaked at the top of the core (see Figure 8). The power distributions and K_{eff} values are acceptable through the first burnup period. During the third period, when control rods are withdrawn from the bottom five fuel regions, the axial power distributions are less ideal, but acceptable (see Figure 8). That is, these power distributions lead to acceptable axial temperature profiles. These power distributions are reasonably stable

Table 6. Results from Multi-Region Control Rod Withdrawal Investigations

Yearly Rod Conditions

Period	Beginning of Period Rod Number Density ($\times 10^{24}$)	Fuel Regions (and Normalized Axial Position) in which Rod is Inserted
1	$8.60\ 10^{-5}$	1-8 (0.0-1.0)
2	$8.56\ 10^{-5}$ (Avg.)	1-5 (0.0-0.62)
3	$8.52\ 10^{-5}$ (Avg.)	1-3 (0.0-0.37)

Reactor Parameters

Period	Time Step	Days	K_{eff}	Max. Axial Peaking Factor	Normalized Axial Position of Max. Power
1	-1	0	1.0369	2.55	0.00
	0	2	1.0098	2.33	0.00
	1	33	0.9993	2.12	0.00
	2	67	0.9984	2.20	0.00
	3	100	0.9965	2.13	0.00
2	-1	100	1.0153	3.04	1.00
	0	102	1.0039	1.60	1.00
	1	133	1.0081	2.23	0.00
	2	167	1.0005	1.84	1.00
	3	200	1.0046	2.34	0.13
3	-1	200	1.0182	1.65	0.41
	0	202	1.0160	1.62	0.41
	1	231	1.0072	1.41	0.43
	2	262	1.0020	1.42	0.17
	3	292	0.9965	1.37	0.17

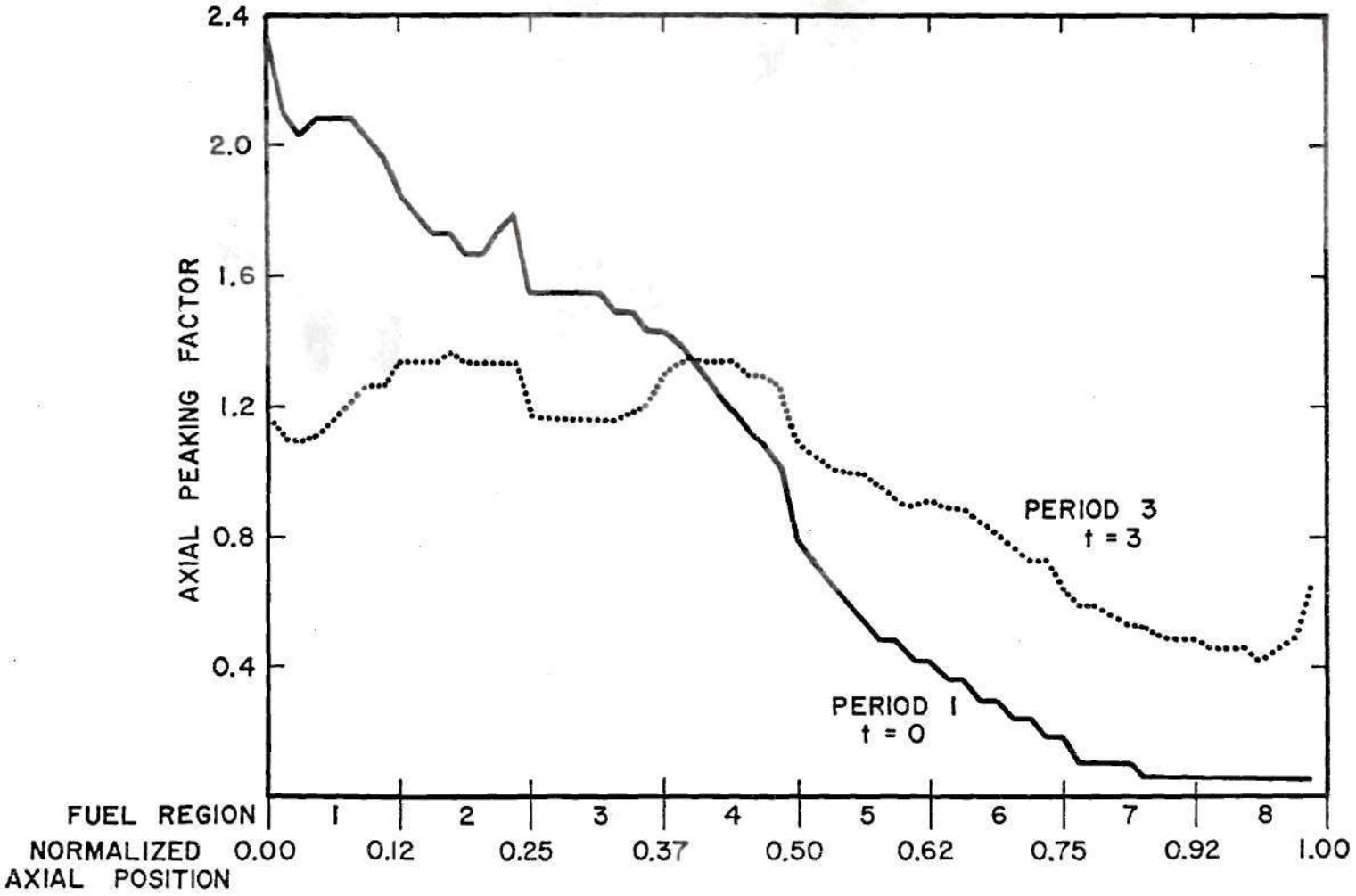

Figure 8. Axial Power Distributions for Multi-region Control Rod Withdrawal Investigations, Periods 1 and 3

throughout the third burnup period. The position of the maximum axial power level does change during the third period, but the overall axial power distributions are relatively steady. Figure 8 shows the axial peaking factors for the first period at t = 0, and for the third period at t = 3. During the second period, when the control rods are withdrawn from three regions, the axial power distributions appear to be unacceptable, when 33 day time steps are used. The power distributions do not approximate the desired exponential shape and they are apparently highly unstable. For the second time period, at t = -1, 0, and 2, the axial power distributions are slightly peaked at the bottom of the core. At time steps t = 1 and 3, the peak power levels occur at the top of the core. Within this 100 day time period, the peak power level shifts from one end of the core to the other three times. A fuel scheme with such unstable axial power distributions would be difficult to control. Also, these axial power distributions would lead to unacceptably high peak fuel temperatures.

Further investigations were done to determine the effect of reducing the length of the time steps during the second time period (when power oscillations were observed). Immediately following the partial rod withdrawal, calculations were made for 40 time steps of 1.929 hours each. During this period, short-term power oscillations due to oscillation in the Xe^{135} concentration were anticipated. These (convergent) oscillations were observed, as shown in Figure 9; similar power oscillations are discussed in the appendix. Following the 77.2 hours of short time steps, calculations were made for 25 time steps of 3 days each. Figure 9 shows the axial peaking factors at the top of the core, immediately before partial rod withdrawal and as a function of time after partial rod withdrawal. Also shown on this figure are the top-of-core axial peaking factors which

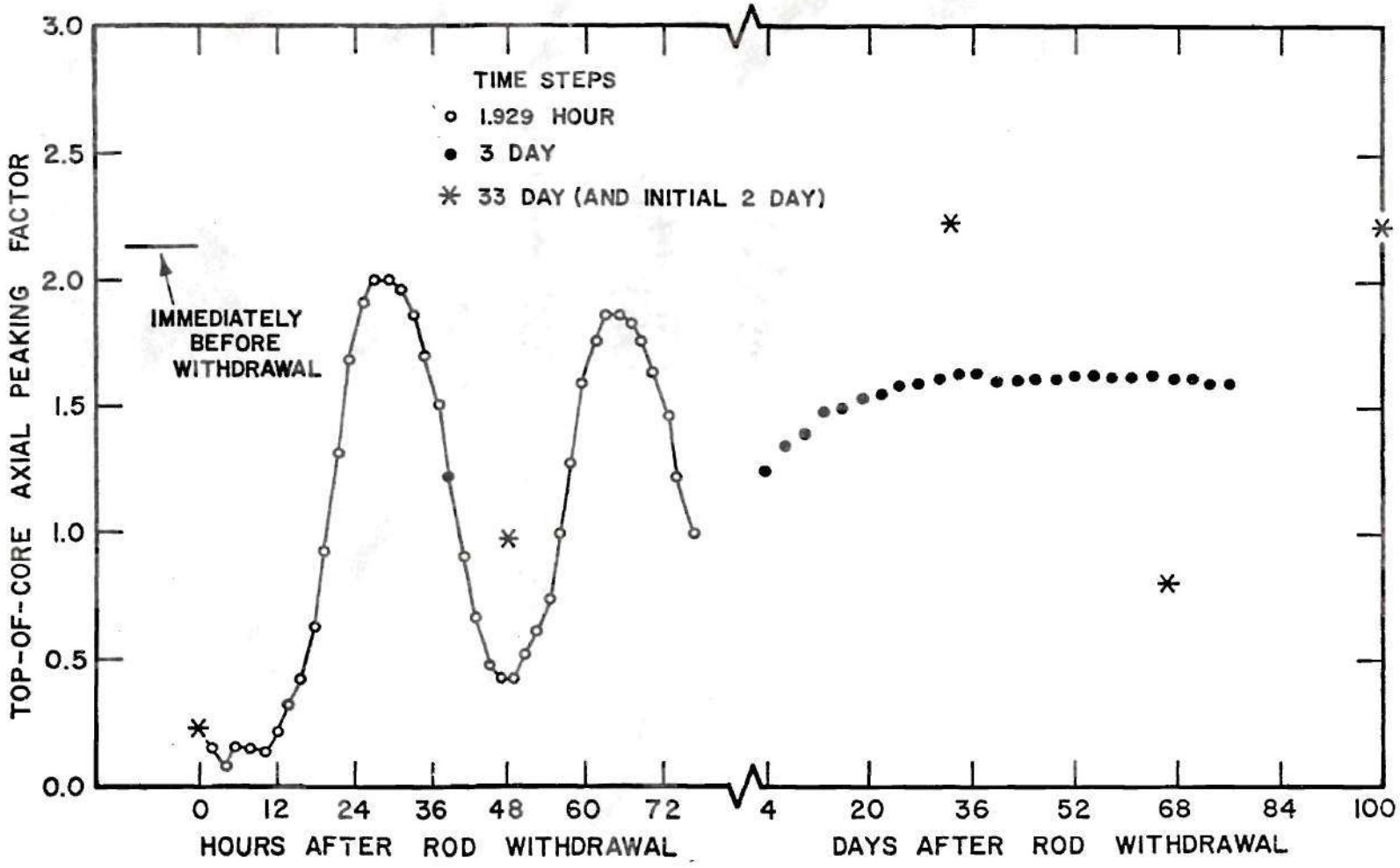

Figure 9. Top-of-core Axial Peaking Factors for Multi-region Control Rod Withdrawal Investigations, Period 2

were calculated using the longer 33 day time steps.

These results indicate that this partial rod withdrawal does not induce long-term power oscillations. Rather, short-term convergent oscillations are induced immediately following partial rod withdrawal; after about 7 days, however, the power distribution was quite stable, as shown in Figure 9. It is not clear why there is such a discrepancy between the two trials (33 day versus 3 day time steps). However, the latter should be a more accurate representation. Not only is there a shorter depletion period between calculations, but the initial xenon buildup is "followed" in 40 steps of 1.929 hours, for the latter trial. For the former trial, the initial xenon buildup is "followed," only by a single 2 day time step, and this does not fully represent the initial oscillation.

Single Region Rod Withdrawal. The following investigations were done to determine if a more gradual control rod withdrawal would result in more stable and more acceptable axial power distributions for this fuel scheme. The aged fuel concentrations from the last time step of the previous fuel cycle year, together with the fresh reload fuel concentrations, were used to begin this yearly fuel cycle investigation. For the first period of this year, control rods were fully inserted into all the fuel regions, as before. The reactor parameters were very similar to those of the previous fuel cycle year, for this first period. The control rod was then withdrawn in three 33.33 day periods, each with time steps of 11.11 days. At the beginning of each of these periods, the rod was withdrawn from one fuel region. Finally, the control rod was withdrawn through the fifth and fourth fuel regions in two 46.1 day periods (with 15.367 day

time steps). Thus, at the beginning of each of these last five periods (periods 2 through 6) the rod was withdrawn from one fuel region. The reactor parameters at each of the time steps are summarized in Table 7. Again, the reactor parameters at time step -1 are not very significant.

These results indicate that the withdrawal of the control rod through a single region at each time period results in stable axial power distributions, i.e., there is no oscillation in these power distributions, as there was before. These power distributions are nearly constant throughout burnup, except for a transition from time step 0 to time step 1 during period 5. This change occurs immediately after the control rod is withdrawn from an axial region with a relatively high power level. After the control rod was withdrawn from region 5, at time steps -1 and 0, the peak power level occurred at the boundary between regions 5 and 6 (normalized axial position of 0.63). For the following time steps the power levels in regions 5 and 6 are reduced by about 20 percent, and the peak power levels occur near the top of the core.

One reason for this transition is the redistribution of Pa^{233}, which results from neutron capture in Th^{232}. Pa^{233} has a 27 day half-life. In this fuel scheme, the Pa^{233} neutron absorption to production ratio is about 80. Because of this large ratio, a local increase in the Pa^{233} concentration serves to depress the local power level. From time step 0 to time step 1 (13 days), the Pa^{233} concentration decreases in regions 1-3 and the power level increases there; conversely, the concentration increases in regions 4-8, and the power level decreases there. By time step 2 (30.73 days after rod removal) the Pa^{233} concentration is changing at a

Table 7. Results from Single Region Control Rod Withdrawal Investigations

Period	Fuel regions (and normalized position) in which rod is inserted	Time step	Days	K_{eff}	Max. axial peaking factor	Normalized axial position of max. power
1	1-8	-1	0	1.0380	2.41	0.00
	(0.00 - 1.00)	0	2	1.0112	2.20	0.00
		1	33	1.0008	2.02	0.00
		2	67	0.9999	2.13	0.00
		3	100	0.9982	2.07	0.00
2	1-7	-1	100	0.9988	1.78	0.00
	(0.00 - 0.87)	0	102	0.9990	1.95	0.00
		1	111	0.9985	1.93	0.00
		2	122	0.9978	1.95	0.13
		3	133	0.9968	1.96	0.13
3	1-6	-1	133	1.0001	1.95	1.00
	(0.00 - 0.75)	0	135	0.9991	1.71	0.13
		1	144	0.9983	1.72	0.13
		2	155	0.9975	1.80	0.13
		3	167	0.9961	1.78	0.13
4	1-5	-1	167	1.0033	1.69	1.00
	(0.00 - 0.62)	0	169	1.0013	1.25	0.14
		1	178	1.0006	1.61	0.13
		2	189	0.9988	1.45	0.14
		3	200	0.9977	1.64	0.13
5	1-4	-1	200	1.0058	1.31	0.63
	(0.00 - 0.50)	0	202	1.0053	1.23	0.63
		1	215	1.0029	1.42	0.14
		2	230	1.0003	1.30	0.16
		3	246	0.9980	1.43	0.14

Table 7. Continued

Period	Fuel regions (and normalized position) in which rod is inserted	Time step	Days	K_{eff}	Max. axial peaking factor	Normalized axial position of max. power
6	1-3 (0.00 - 0.37)	-1	246	1.0097	1.54	0.44
		0	248	1.0092	1.51	0.44
		1	261	1.0057	1.41	0.44
		2	276	1.0028	1.38	0.44
		3	292	1.0000	1.35	0.44

much slower rate, and the power distributions are nearly constant. It should be noted that this transition represents a much smaller power change than the oscillations observed previously. Also, the resulting axial temperatures are acceptable at all time steps during period 5.

The stability of the axial power distributions and the range of the K_{eff} values seem acceptable, under the single region withdrawal pattern. The acceptability of the axial temperature profiles which result from these power distributions will be discussed later.

Half Region Rod Withdrawal. A final set of control rod investigations was done to determine if a more gradual rod withdrawal rate during periods 4 and 5 would reduce the previously discussed power transition. The control rod withdrawal through regions 6 and 5 was done in four periods. These new periods of withdrawal will be designated 4(1), 4(2), 5(1), and 5(2) to correspond to periods 4 and 5 shown in Table 7. These investigations begin with the nuclide concentrations at the beginning of period 4 from the previous fuel cycle year. At the beginning of period 4(1), the control rod concentration in region 6 is reduced by one half, corresponding to the withdrawal of the rod halfway through this region. (Note, however, that the reduced control rod concentration is considered to be homogeneously distributed throughout region 6). At the beginning of period 4(2), the control rod is completely withdrawn from region 6. These new periods (and their time steps) are about one half as long as those of the previous investigation. Likewise, the control rod concentration is reduced by one half in region 5 at the beginning of period 5(1), and the rod is withdrawn from region 5 at the beginning of period 5(2). The resulting reactor parameters are shown in Table 8.

Table 8. Results from Half-region Control Rod Withdrawal Investigations

Period	Regions with full rod insertion	Regions with half-rod insertion	Time step	K_{eff}	Max. axial peaking factor	Normalized axial position of max. power
4(1)	1-5	6	-1	0.9981	1.37	0.14
(16.67 days)			0	0.9979	1.58	0.13
			1	0.9975	1.63	0.13
			2	0.9968	1.64	0.13
			3	0.9962	1.66	0.13
4(2)	1-5	---	-1	0.9996	1.33	1.00
(16.67 days)			0	0.9991	1.37	0.14
			1	0.9986	1.48	0.14
			2	0.9978	1.48	0.14
			3	0.9972	1.53	0.14
5(1)	1-4	5	-1	1.0003	1.26	0.16
(15.37 days)			0	1.0001	1.32	0.16
			1	0.9995	1.40	0.14
			2	0.9988	1.41	0.14
			3	0.9981	1.44	0.14
5(2)	1-4	---	-1	1.0027	1.24	0.63
(15.37 days)			0	1.0024	1.20	0.17
			1	1.0015	1.28	0.16
			2	1.0007	1.29	0.16
			3	0.9999	1.33	0.16

For the half-region withdrawal pattern, all the reactor parameters are favorable. The range of K_{eff} values is small for each period. The axial power distributions are very stable; the transition which previously occurred at the beginning of period 5 is no longer present. Again, however, the merit of these power distributions is primarily determined by the thermal analysis results.

Thermal Analysis

POKE

POKE is a computer code which determines the steady state coolant mass flow, coolant temperature, and fuel temperature distributions in a gas-cooled reactor. Input to POKE includes fuel element geometry and arrangement, coolant and fuel material data, total reactor power, helium inlet temperature, and pressure. A power distribution is also input by giving the radial peaking factors, and the axial power distribution of the core.

The reactor configuration treated by POKE consists of a number of parallel radial fuel regions connected to common inlet (top) and outlet (bottom) plenums. The fuel regions extend in the axial direction. Between the plenums, the radial fuel regions consist of a top reflector, the eight axial fuel regions of the core, and a bottom reflector. For each radial fuel region the following are specified by the user: the region's radial peaking factor; the number, size, and geometry of both the coolant channels and the fuel holes; and the radial arrangement of coolant channels and fuel holes. The coolant channels run continuously from inlet plenum to outlet plenum.

In these investigations, the core conditions which are specified are those of a 1100 MW(e) HTGR applicable to process heat applications. The calculations are made for each of 33 radial fuel regions. These 33 regions have specified radial peaking factors ranging from 0.4 to 1.4. For an axial fuel shuffling scheme it is estimated, however, that the maximum radial peaking factor will be 1.2. The axial power distributions which were determined by the FEVER investigations are used for each radial fuel region. Other reactor operating conditions which are input to the code are listed below.

Reactor Operating Conditions for 1100 MW(e) HTGR
Applicable to Process Heat Applications

Coolant (Helium) Pressures (psia)

Region Inlet - 700.0

Region Outlet - 696.0

Coolant Temperatures ($^{\circ}$F)

Region Inlet - 650.0

Region Outlet - 1850.0

Coolant Flow Rate (lb/sec)

Total Reactor - 1986.1

The analysis performed by POKE consists of an iterative solution of three one-dimensional (axial) equations which express the conservation of mass, momentum, and energy for each radial fuel region modelled. The output from this code is calculated for a specified number of axial positions, for each region. In this investigation there are 33 evenly spaced

positions along the axial fuel column at which calculations are made. Position-dependent output includes: coolant temperature, coolant channel surface temperature, and maximum (center-line) and minimum fuel rod temperatures.

Note that for this investigation the process heat HTGR's physical specifications and many of the operating conditions are assumed fixed. The only input variable which is determined by the fuel scheme is the normalized axial power distribution. In effect, this code determines the temperature level of the fuel, as a function of axial position for any axial power distribution, which is required to yield the specified fuel region power production. The required regionwise power production is equal to the specified average region power level times the region's radial peaking factor. For the optimum axial power distribution, the axial fuel temperature profile is flat in each radial fuel region. For the conditions specified for the process heat HTGR, the optimum axial power distribution yields a constant axial fuel temperature profile with a maximum fuel temperature of about 2190 °F in a fuel region with a radial peaking factor of 1.2 (and "local power tilt" = 1.0). All other axial power distributions yield a higher maximum axial fuel temperature for this region, at these specified operating conditions. It is required that the maximum axial fuel temperature be limited to insure the integrity of the fuel materials.

After the thermal calculations have been made for each radial fuel region, the user can specify that "subregion" thermal analysis be done for individual radial fuel regions. Subregion analysis makes it possible to

account for flow and power imbalances within an individual fuel region due to local power tilts. The individual radial fuel region is divided into a specified number of radial subregions, which extend the total axial length of the core, and thermal calculations are made for each subregion. A "local power tilt" is specified for each subregion; the local power tilt is equal to the power density (power per unit volume) of the given subregion divided by the average power density of that region. Thus, the local power level at any specified position in the core is equal to the product of: the average radial region power level, the specified region's radial peaking factor, the axial peaking factor of the specified position, and the local power tilt of the specified subregion. The average radial region power level is equal to the specified total core power divided by the number of radial fuel regions. The axial peaking factors which are used for each radial fuel region (and each subregion) are those which were determined in the FEVER investigations.

For the fuel regions of the proposed HTGR, it is estimated that the maximum local power tilt will be 1.2. Thus, the maximum possible power level would occur in a subregion with a local power tilt of 1.2, which is located within a region which has a radial peaking factor of 1.2. This will be the "hot channel" subregion with the maximum local center-line fuel temperature. For the ideal axial power distribution, the maximum steady-state center-line fuel temperature is 2536 °F. For the process heat HTGR, operating at full-power steady-state conditions, it is required that the maximum local center-line fuel temperature be limited to about 2850 °F.

Results

For the fully inserted control rod investigations of the Trial 8 fuel scheme, thermal analyses were done at the following times: Beginning of Cycle (BOC) at t = 0 of the first time period, Middle of Cycle (MOC) at t = 1 of the second time period, and End of Cycle (EOC) at t = 3 of the third time period. The thermal analyses were done for three fuel cycle years. The maximum local center-line fuel temperatures are recorded in Table 9. The axial center-line fuel temperature profiles for the third fuel cycle year at BOC and EOC are shown in Figure 10. These temperature profiles are for the hot channel subregion. The discontinuities in these temperature profiles are primarily due to discontinuities in the axial power distributions. Axial power distributions were calculated by the FEVER code, and the power discontinuities were caused by differences in the fuel concentrations of adjacent axial fuel regions. Also shown in this figure is the temperature profile which results from the ideal axial power distribution (see Figure 7).

Note that for the second and third years, the BOC and MOC maximum temperature levels are above the limit of 2850 °F. These excessive temperatures all occur in the top quarter of the core, indicating that the power densities there are too large at these times. In each case, the excessive temperature occurs at a position where the axial peaking factor exceeds the axial peaking factor of the ideal power distribution by at least 20 percent.

Thermal analyses were next done for the multi-region rod withdrawal trials, which were summarized in Table 6. The time steps at which the

Table 9. Thermal Analyses of Fully Inserted Rod Investigations

Year	Period	Time step	Max. local center-line fuel temp. (°F)	Normalized axial position of max. temp.
1	1	0	2768	0.25
1	2	1	2852	0.25
1	3	3	2600	1.00
2	1	0	2901	0.10
2	2	1	2911	0.25
2	3	3	2631	1.00
3	1	0	3033	0.10
3	2	1	2950	0.25
3	3	3	2628	0.25

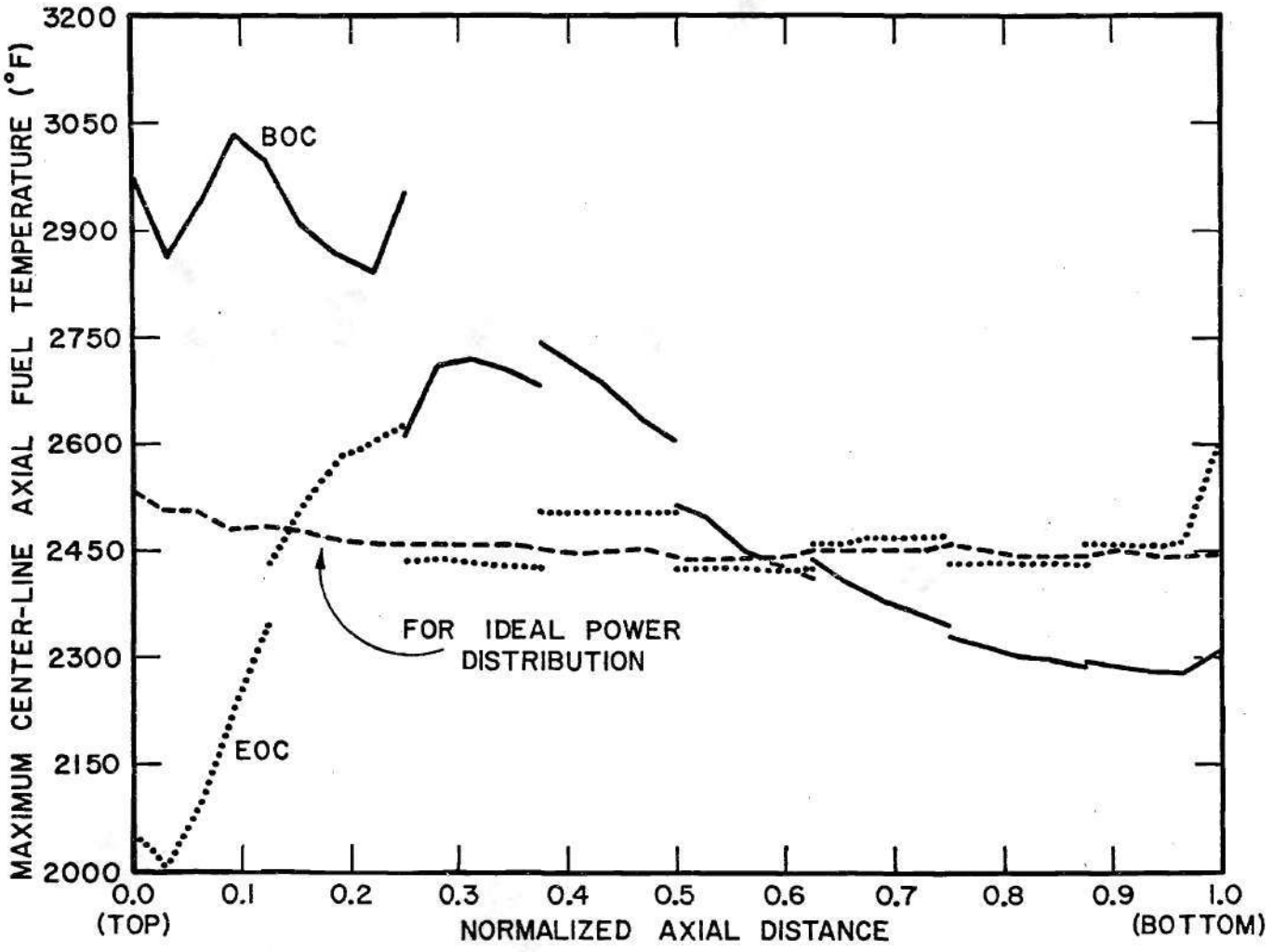

Figure 10. Axial Temperature Profiles for Fully Inserted Rod Investigations

analyses were done and the results are summarized in Table 10. The time steps chosen were those at which the axial power distributions deviated most from the ideal power distribution. These were the time steps at which the maximum yearly center-line fuel temperatures were expected. During period 2, thermal analyses were done for the axial power distributions from the trials using 3 day time steps (see Figure 9). Temperature profiles were determined at the end of the first 3 day time step, and again at the end of the last 3 day time step (78.8 hours after partial rod withdrawal). The maximum temperature levels for this control pattern occurred at the beginning of period 1.

Thermal analyses were next done for the single region control rod withdrawal trials, which were summarized in Table 7. The time steps at which the analyses were done and the results are summarized in Table 10. Again, the time steps were chosen in order to determine the maximum yearly temperatures. For this more gradual withdrawal pattern, only two of the resulting temperatures exceeded the specified limit (by only 19° and 22°).

Finally, thermal analyses were done for the half-region control rod withdrawal trials, which were summarized in Table 8. These results are also summarized in Table 10. Note that the temperatures resulting from this more gradual rod withdrawal pattern are lower than the corresponding temperatures resulting from the single region withdrawal pattern.

Table 10. Thermal Analyses of Partially Inserted Rod Investigations

	Period	Time step	Max. local center-line fuel temp. (°F)	Normalized axial position of max. temp.
Multi-region Rod Withdrawal Trials	1	0	2923	0.37
	2	First 3-day step	2884	1.00
	2	Last 3-day step	2753	0.25
	3	0	2915	0.50
	3	2	2715	1.00
	3	3	2706	0.50
Single Region Rod Withdrawal Trials	1	0	2869	0.37
	2	0	2780	0.25
	3	2	2791	1.00
	4	0	2872	1.00
	4	2	2825	1.00
	5	0	2725	0.75
	5	1	2768	1.00
	6	1	2706	1.00
Half-region Rod Withdrawal Trials	4(1)	0	2742	1.00
	4(2)	0	2806	1.00
	5(1)	0	2714	1.00
	5(2)	0	2711	0.75

CHAPTER IV

CONCLUSIONS AND RECOMMENDATIONS

Summary and Conclusions

Several axial push through fuel schemes were investigated in this project. From the initial unrodded investigations, a fuel scheme with a carbon-to-thorium ratio of 185 appeared most favorable with respect to the range of K_{eff} values, and the stability and acceptability of the axial power distributions. This fuel scheme was further investigated under the conditions of fully and partially inserted control rods. With a fully inserted control rod pattern, the resulting axial power distributions were very stable throughout each burnup period. However, at the BOC and MOC periods, the axial power distributions produced unacceptably high center-line fuel temperatures. Next, a partially inserted control rod pattern was investigated in which the rod was withdrawn in only two steps. The first withdrawal step, from the bottom three fuel regions, resulted in grossly unstable axial power distributions when calculations were made with 33 day time steps. This rod withdrawal was repeated with shorter time steps, to give a more accurate representation. With the shorter time steps, there were initial short-term oscillations (due to xenon), but the long-term power distributions were quite stable. A more gradual control rod withdrawal pattern was investigated next, in which the rod was withdrawn from one axial fuel region at each of five yearly time periods. This control pattern resulted in stable axial power distri-

butions. However, there was a transition in the power distribution after the removal of the rod from the fifth axial fuel region. The maximum center-line fuel temperature resulting from this control pattern was 2872°F, occurring after the rod was removed from the fifth axial fuel region. Finally, an even more gradual rod withdrawal pattern was investigated during the periods the rod was withdrawn from the fifth and sixth axial fuel regions. The rod was removed from each of these regions in two steps. The resulting axial power distributions were steady, without transitions. The resulting maximum center-line fuel temperature was 2806°F for these periods. The results of the single region and half-region rod withdrawal patterns indicate that the maximum yearly center-line fuel temperature is 2869°F for this fuel scheme. This temperature occurs at BOC, in the top half of the core.

These investigations show that a more gradual rod withdrawal rate results in more stable axial power distributions and reduced maximum center-line fuel temperatures.

For the fuel scheme investigated, the maximum fuel temperature occurs in the top half of the core at BOC. At BOC, the top of the core is heavily loaded with fresh fuel. This results in axial peaking factors in the top half of the core which are larger than those of the ideal axial power distribution. For an axial push through pattern, fuel is most rapidly depleted from these heavily fueled regions at the top of the core during the BOC period. Thus, a decreasing fraction of the fuel load is located in the top half of the core during the later periods of the fuel year. This results in a decrease in the top-of-core axial peaking factors and an increase in the bottom-of-core axial peaking factors, throughout

the fuel cycle year. These yearly changes in the axial peaking factors are further increased by the partial withdrawal of control rods. When the control rod is partially withdrawn, in the MOC and EOC periods, it serves to increase the power level in the bottom of the core. Since the total power level is kept constant, the power level and axial peaking factors in the top of the core are reduced following rod withdrawal. For example, in the trials summarized in Table 7, the top-of-core axial peaking factor decreased from 2.20 at BOC to 1.06 at EOC. The bottom-of-core axial peaking factor increased from 0.07 at BOC to 0.54 at EOC.

These investigations indicate that an axial power distribution with higher-than-ideal axial peaking factors in the top half of the core leads to greater fuel temperatures than a power distribution with higher-than-ideal axial peaking factors in the bottom half of the core. For example, in the trials summarized in Tables 7 and 10, a BOC temperature of 2869°F occurred in the top half of the core, at a point where the axial peaking factor was 37 percent greater than the peaking factor of the ideal power distribution. An EOC peak temperature of only 2706°F occurred at the bottom of the core, where the axial peaking factor was 69 percent greater than the peaking factor of the ideal power distribution. Thus, the axial push through pattern leads to maximum fuel temperatures at the top of the core during BOC. Therefore, it is important to obtain the best possible approximation to the ideal power distribution at BOC, in order to reduce the maximum yearly fuel temperature.

Further investigations were done to determine the effects of large instantaneous rod motions on this fuel scheme. The results of these investigations are given in the appendix.

It is acknowledged that this project was based upon nuclear and thermal analyses and that a complete study should include an economic evaluation of any fuel scheme considered.

Recommendations

1. Fuel scheme investigations similar to those described herein could be done with variations in any of the following parameters: fresh fuel concentrations, fuel residence time, shuffle scheme, and the number of axial fuel regions. The most important fuel concentration variables are the amount and isotopic composition of uranium and the amount of thorium. Longer fuel residence times (e.g., six years) should also be considered. Note that, for the fuel scheme investigated, the control rods are not fully withdrawn at EOC; thus the fuel is not being fully depleted before removal from the core. By either reducing the fresh fuel load or by lengthening the fuel cycle time, the fuel could be more fully depleted before it is removed at EOC. Also, there are many fuel placement schemes other than axial push through which can be investigated. Likewise, variation could be made in the size of the axial fuel column. If longer columns (e.g., ten axial fuel regions) were used, it should be possible to obtain the same exit helium temperature with a reduction in the required linear power density and the maximum fuel temperature.

2. Because of the findings mentioned previously in this chapter, it is suggested that the shape of the axial power distribution at MOC and EOC are not of critical importance. Further investigations should primarily consider the shape of the axial power distribution at BOC. Maximum yearly fuel temperature levels are not expected at MOC and EOC

for the axial push through scheme.

3. Further investigations could be done to determine the effect of the time step size on the FEVER calculations. The results herein indicate that large time steps (e.g., 33 days) are not adequate for calculations following a large perturbation of the reactor power level.

4. Further investigations, such as those described in the appendix, could be done regarding possible power oscillations due to large instantaneous rod motion. It should be determined if there is a "threshold" for power oscillations for either rod withdrawal or rod insertion. Also, the maximum power oscillation and the conditions producing it should be determined for any fuel scheme considered.

5. The following recommendation is made regarding the utilization and/or possible modification of the FEVER code. Future users should investigate the "Control Search" option of this code; this could be especially helpful during the initial control-rodded trials. Ideally, this code would allow several control-rodded trials to be run in succession. First, the control option could be used to find the control rod number density which is required to yield an initial K_{eff} value specified by the user. With this control rod number density, burnup calculations would be done until K_{eff} dropped below another specified (subcritical) value. Ideally, the code would then calculate the rod withdrawal which is required to re-establish a specified (slightly supercritical) K_{eff} value. Such calculations of burnup period and required rod withdrawal could be done successively until the completion of the fuel cycle year.

APPENDIX

XENON OSCILLATION TRIALS

Two final investigations which simulate large instantaneous changes in control rod placement were carried out. These were done to determine the behavior of this fuel cycle after an instantaneous removal of the control rod and the reinsertion of the rod after 13.5 hours of unrodded operation. The nuclide concentrations from period 4(1) at time step 3 (Table 8) were used to begin this trial. During period 4(1), the control rod was fully inserted into the top five axial fuel regions and "half-inserted" into the sixth fuel region.

For the first part of the xenon oscillation trials, the control rod was completely withdrawn from the core, and the reactor parameters were determined for 20 periods of 1.929 hours each. Rod withdrawal raised the K_{eff} value by 0.0690, from 0.9962 to 1.0652. The resulting axial power distributions were not oscillatory, as shown in Figure 11. This figure shows the maximum axial peaking factors in region 1 (top of the core) and region 6 (in the bottom half of the core) as a function of time. The maximum axial peaking factors immediately before rod removal are also shown. Following rod removal from the top of the core, the axial power distributions were more steeply peaked toward the top of the core. Immediately before rod removal, the maximum axial peaking factor was 1.66, occurring near the top of the core. Immediately after rod removal, the maximum axial peaking factor was 2.88, occurring at the top of

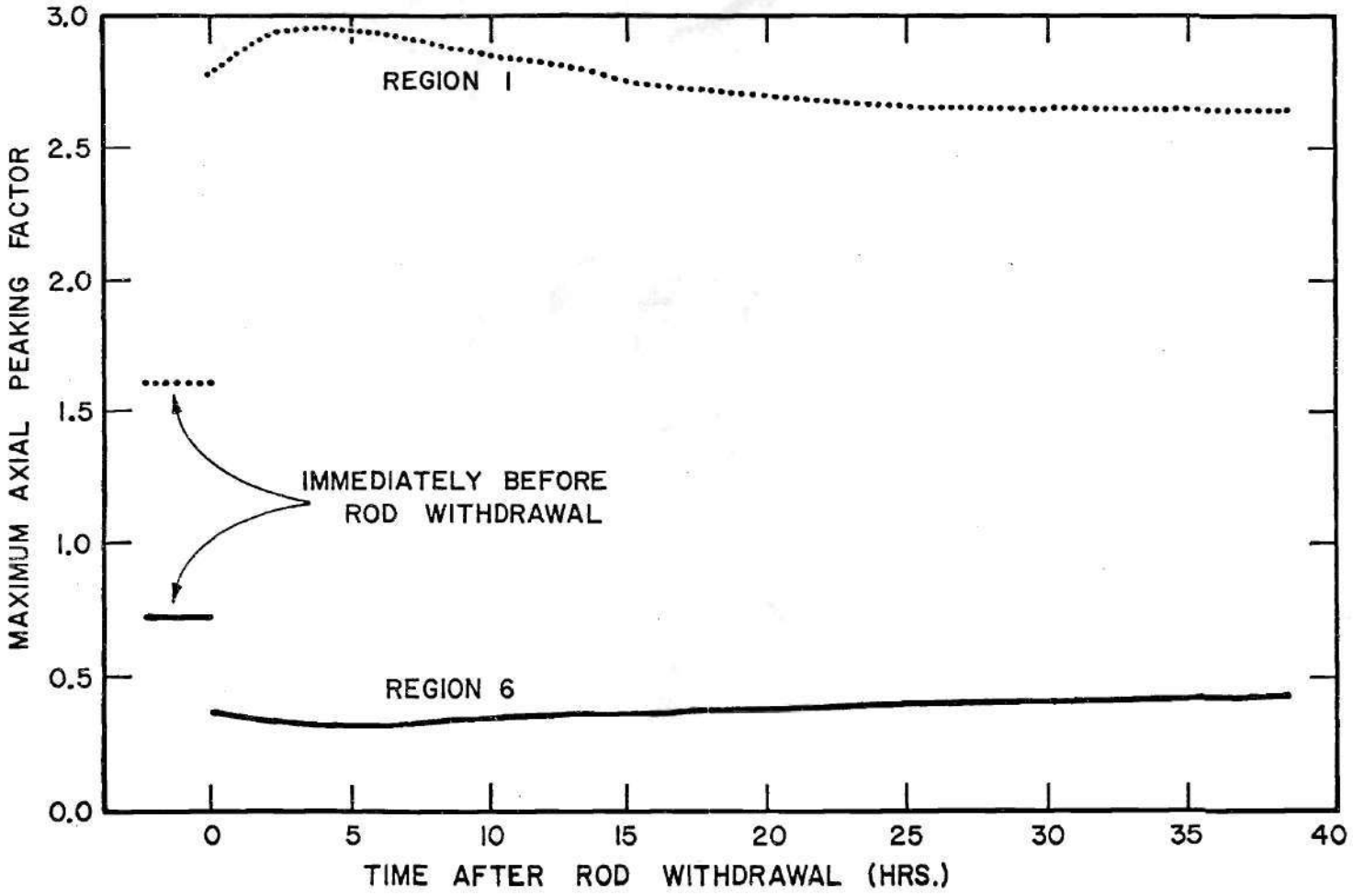

Figure 11. Peaking Factors versus Time Following Control Rod Removal

the core. This rod removal thus served to further increase the already relatively high power levels in the fuel regions at the top of the core. The results indicate that this perturbation does not induce oscillations in the axial power distributions.

The nuclide concentrations from time step 7 (after 13.5 hours of unrodded operation) were used to begin the second part of this trial. The rod was reinserted into the top five axial fuel regions, and the reactor parameters were determined for 45 time steps of 1.929 hours each. Rod reinsertion reduced the K_{eff} value by 0.0676, from 1.0657 to 0.9981. The resulting oscillation in the axial power distributions can be seen in Figure 12. This figure shows the maximum axial peaking factors in the first and sixth fuel regions as a function of time. The maximum axial peaking factor for the total core occurred in region 6 during time steps 1 through 8 (2 hours through 16 hours) and in region 1 at all other time steps. Also shown are the axial peaking factors immediately before rod reinsertion. In both regions, the power distributions oscillate out of phase with the changes in the Xe-135 concentrations. For example, in region 1 the Xe-135 concentration is reduced by a factor of 2.18 from time step 4 (at 8 hours) to time step 14 (at 27 hours), while in region 6 the concentration increases by a factor of 1.92. Xenon-135 is the only nuclide whose change in concentration is significant during these short time steps. As can be seen in Figure 12, the axial power oscillation which was induced by this rapid rod insertion is convergent for this fuel scheme.

In contrast to rod withdrawal, this rod insertion induced changes

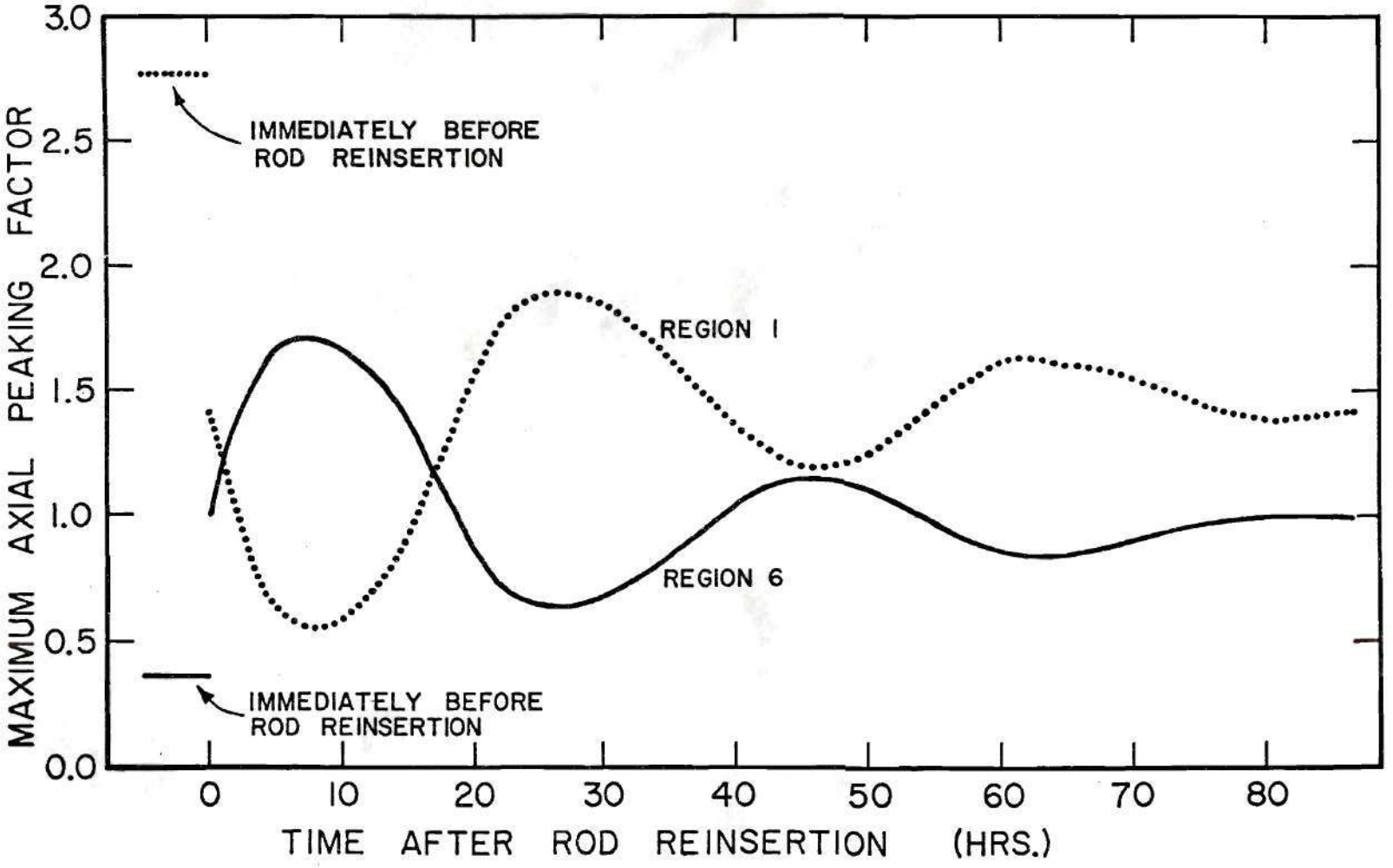

Figure 12. Peaking Factors versus Time Following Control Rod Reinsertion

in the axial power distribution which did not "enforce" the existing power shape. That is, this rod insertion caused a decrease in the relatively high power levels at the top of the core. As shown, this perturbation induced a convergent oscillation in the axial power distribution. These results indicate that the generation of a power oscillation is dependent upon the direction of rod motion.

It is suggested that further trials be done to determine if there is a "threshold" magnitude of rod motion for which a power oscillation is induced for this fuel scheme or similar schemes. If there is a threshold for the case of rod withdrawal, it is apparently much larger than for the case of rod reinsertion. That is, rod withdrawal through a larger number of fuel regions would be required to induce an oscillation.

BIBLIOGRAPHY

Literature Cited

1. F. W. Todt and L. J. Todt, FEVER/M1 A One-Dimensional Depletion Program for Reactor Fuel Cycle Analysis, Gulf General Atomic Company Report GA-9780 (1969).

2. W. Pfeiffer, G. Malek, and K. Lund, POKE A Gas-Cooled Reactor Flow and Thermal Analysis Code, Gulf General Atomic Company Report GA-10226 (1970).

3. U. S. Atomic Energy Commission Report WASH-1085 (1969), p. 12.

4. R. C. Dahlberg (GGA), Private Communication, 1971.

5. See reference 4.

6. See reference 4.

7. See reference 4.

Other References

R. C. Dahlberg, R. F. Turner, and W. V. Goeddel, "Core Design Characteristics," Nuclear Engineering International, December 1969.

L. J. Colby, R. C. Dahlberg, and S. Jaye, HTGR Fuel and Fuel Cycle Summary Description, Gulf General Atomic Company Report GA-10233 (1971).

A. J. Goodjohn and D. B. Trauger, Special Development Problems of HTGR Systems, Gulf General Atomic Company Report GA-10265 (1970).